RF Energy Harvesting in a Decode-and-Forward Wireless Relay Network

by

Lina Elmorshedy

B.Sc., Faculty of Engineering, Alexandria University, 2008

A THESIS SUBMITTED IN PARTIAL FULFILLMENT OF
THE REQUIREMENTS FOR THE DEGREE OF

MASTER OF APPLIED SCIENCE

in

The Faculty of Graduate and Postdoctoral Studies

(Electrical and Computer Engineering)

THE UNIVERSITY OF BRITISH COLUMBIA

(Vancouver)

April 2016

Abstract

Wireless communication has experienced tremendous growth over the past three decades. This led to the development of many novel technologies aimed at enhancing the system performance due to the limited availability of radio resources. Cooperative relaying is a promising technology which enhances transmission reliability using simple hardware. However, the extra power consumed for the process of information relaying may be an issue. Recent advances in wireless energy transfer have made it possible for self-sustainable relays that power themselves by capturing ambient energy wirelessly. In this thesis we focus on two technologies, namely, cooperative relaying which enhances the energy efficiency and reliability by allowing multi-hop communication with low power nodes, and Radio Frequency (RF) energy harvesting which obviates the need for a battery by capturing the ambient RF energy and using it as a source power.

In the first part of the thesis, we study RF energy harvesting in a Decode-and-Forward (DF) Wireless Relay Network (WRN) in the presence of an interferer node. We consider the Time Switching Relaying (TSR) protocol, the Power Splitting Relaying (PSR) protocol and we propose a new hybrid TSR-PSR protocol. We derive expressions for the outage probability and throughput in the delay-sensitive transmission mode for the three relaying protocols, and compare their performances. For simplicity, we neglect the energy harvested from the interferer signal.

In the second part, we study the general case in which we include the effect

of harvesting energy from the interferer signal. Expressions for the outage proba-
bility and throughput in the delay-sensitive transmission mode are derived for the
three relaying protocols. Numerical results are presented to illustrate the effect of
including RF energy harvesting from the interferer.

In the third part, we study shared and non-shared power allocation schemes for
a two-hop DF WRN with multiple source-destination pairs. The pairs communicate
via a single relay which harvests RF energy from the source transmissions in the
presence of an interfering signal. The studied schemes are compared in terms of out-
age probability, throughput in the delay-sensitive transmission mode and fairness.

Preface

Chapter 2 is based on a manuscript titled "RF Energy Harvesting in DF Relay Networks in the Presence of an Interfering Signal" that has been accepted for publication in the 2016 IEEE International Conference on Communications (ICC). The manuscript is co-authored by myself as the first author, my supervisor, Dr. Cyril Leung and S. A. Mousavifar, a former PhD student in our group. I was the primary researcher in this work. I came up with the idea of the research independently. My contributions included conducting the literature review, identifying and formulating the research problem, and carrying out the mathematical analysis and simulations under the supervision of Dr. Cyril Leung. S. A. Mousavifar also provided valuable comments and helped me by providing technical and editorial feedback while writing the associated manuscript for publication.

Table of Contents

List of Tables

List of Figures

List of Acronyms

AF   Amplify-and-Forward

CCI   Co-channel Interference

CDF   Cumulative Distribution Function

CSI   Channel State Information

DF   Decode-and-Forward

DS   Dual-Source

EPA   Equal Power Allocation

KKT   Karush-Kuhn-Tucker

MABC   Multiple Access Broadcast

MMRD   Max-Min Relay-Destination rate

NSPA   Non-Shared Power Allocation

pdf   probability density function

PS   Power Splitting

PSR   Power Splitting Relaying

RDCD   Relay-Destination Channel Dependent

RF　　　　　Radio Frequency

rv　　　　　Random Variable

SBS　　　　Single-Best-Source

SFS　　　　Single-Fixed-Source

SIR　　　　Signal to Interference Ratio

SNR　　　　Signal to Noise Ratio

SWIPT　　Simultaneous Wireless Information and Power Transfer

TDBC　　　Time Division Broadcast

TS　　　　　Time Switching

TSR　　　　Time Switching Relaying

TWRN　　　Two-Way Relay Network

WRN　　　　Wireless Relay Network

WSN　　　　Wireless Sensor Network

WSRM　　　Weighted-Sum-Rate Maximization

List of Symbols

α	The time switching ratio
γ_{th}	The SIR threshold value
Γ_D	The SIR at the destination node
Γ_R	The SIR at the relay node
η	The energy harvesting efficiency
θ_i	Fraction of total power at relay assigned to link $\mathbf{R} - \mathbf{D}_i$
μ_i	Weight assigned to link $\mathbf{R} - \mathbf{D}_i$
ρ	The power splitting ratio
τ_{ds}	Throughput in the delay-sensitive mode
d_1	Distance from interferer node to relay node
$d_{2,i}$	Distance from interferer node to i-th destination node
$d_{3,i}$	Distance from i-th source node to relay node
$d_{4,i}$	Distance from relay node to i-th destination node
E_{h_r}	Energy harvested at the relay
$Ei(.)$	Exponential integral function
F_I	Fairness index
m	Path loss exponent
N	Number of source-destination pairs
$P_{\mathcal{I}}$	Interferer transmit power
P_{out}	Outage probability

P_r	Relay transmit power
P_s	Source transmit power
$R_{i,d}$	Data rate at i-th destination
$R_{i,r}$	Data rate from i-th source to relay

Acknowledgements

I would like to express my sincerest gratitude to my supervisor, Professor Cyril Leung, first for accepting me as a Masters student in his group, and most importantly for his continuous support and invaluable guidance throughout my Masters program. I am very much grateful for his time, patience, critical suggestions and helpful comments. Without his immense knowledge and constant encouragement this thesis would have never been possible. I am also thankful to, Seyed Ali Mousavifar, a former PhD student in the data communications group, for his constructive suggestions and helpful advice during my research.

I would like to express my heartfelt gratitude to my biggest supporter, amazing friend and loving husband, Ossama Elmorshedy, who is also my colleague in the Electrical and Computer Engineering department in UBC. His rock solid beliefs in my capabilities have always been my greatest source of motivation throughout our life. Without his unconditional support and love, I would not have been able to complete this thesis. Special thanks to my parents, sister and brother for their support, continuous advice and motivation during the past years.

Last but not least, I would like to express my gratitude to my lab mates for their invaluable support, and friendship during my Masters program. I am also thankful to all my colleagues in the Electrical and Computer Engineering department in UBC for the fun we had in the last two years making my graduate studies such a great experience.

Acknowledgements

Dedication

I dedicate this thesis to my family. My deepest feeling of gratitude goes to my loving mother, Hala Elmorshedy, to whom I owe where I am today. I am grateful for her unconditional sacrifice, relentless support and her continuous words of wisdom and encouragement which have always been my constant guide throughout my life. Many thanks to my sister and best friend, Omniah and my dear brother, Zeyad for their unconditional love and support. My sincerest expression of love and appreciation goes to my husband, Ossama, for his exceptional sacrifice and encouragement throughout my Masters program. I would also like to dedicate this thesis to my daughter and my greatest blessing, Joury, whose presence have been and will always be the biggest inspiration in my whole life.

Chapter 1

Introduction

Wireless communication systems have been experiencing very rapid growth due to the demand for wireless services over the past three decades. An important research objective is to find solutions to meet such increasing demands given the limited availability of radio resources. Cooperative communications allow users within a network to collaborate with each other in the process of information transmission, given the broadcast nature of wireless networks. This can lead to enhanced energy efficiency, improved network connectivity and increased reliability. As a result cooperative communications have been found to improve the performance of resource-constrained wireless networks [1]-[3].

Moreover, the performance of wireless communication systems is constrained by the limited battery life of wireless devices. Hence, energy harvesting has received significant attention recently. Energy harvested from the surrounding environment (i.e. wind, heat, solar, etc.) can be used to prolong the network lifetime, and to eliminate the need for replacing or recharging the batteries of wireless nodes. In many cases, replacing the node batteries may be costly, toxic, undesirable or impractical. More recently energy harvesting from Radio Frequency (RF) signals has been studied as a promising solution to prolong the lifetimes of energy-constrained wireless networks ([4] and references therein).

In this chapter, we briefly present the fundamentals of cooperative relaying, energy harvesting and a basic overview of resource optimization in wireless commu-

nication systems. An outline of the thesis is also provided.

1.1 Cooperative Relaying in Wireless Networks

Cooperative relaying is a novel technology which improves the energy efficiency and the reliability of wireless networks by employing intermediate relay nodes between various source and destination nodes. This allows short distance multi-hop communication with low powered nodes, instead of long distance direct communication with high powered nodes. It provides a larger coverage area and longer network lifetime, thus improving the performance of wireless communication systems.

There are different relaying protocols for cooperative networks such as Amplify-and-Forward (AF) and Decode-and-Forward (DF) [5]. In DF relaying, the relay node receives the signal sent by the source node, decodes it and then forwards it to the destination node. In AF relaying, the relay node receives the signal sent by the source node, amplifies it and then forwards it to the destination node.

1.2 Energy Harvesting in Wireless Networks

Limited device battery life has always been a key concern in the design of wireless communication systems. Energy harvesting has been proposed as a promising solution to that problem, such that energy is captured and stored from external surrounding sources. This technology has received significant attention recently specially with the emergence of miniature electronics devices and low power Wireless Sensor Network (WSN) systems, in which the finite lifetime of the node batteries limits the lifetime of their applications [6]. The benefits of energy harvesting arise in applications where the charging of the batteries is one of the major problems to be addressed, specially when the wireless nodes are located in difficult to access

environments or even inaccessible places, or the number of wireless nodes is quite large and are distributed in a wide area.

Various sources of renewable energy such as solar, mechanical, wind and thermal energy can be used to power wireless communication networks [6]-[8]. However, the main problem of energy harvesting from renewable sources is its random nature. This makes it unreliable since it depends on the energy availability that may vary with location, time and weather conditions. Therefore, it is not easy to predict the amount of energy that can be harvested from the environment which makes resource allocation in such systems a challenging problem.

Recently, wireless energy transfer has been introduced for RF energy harvesting in wireless communication systems through a paradigm referred to as Simultaneous Wireless Information and Power Transfer (SWIPT) [9],[10]. In SWIPT, the RF energy transfer and information transmission are performed in the downlink at the same time, which is possible since RF signals carry both energy and information simultaneously. Therefore the energy-constrained nodes can decode information as well as harvest energy from the received RF signal.

An ideal receiver design which can simultaneously extract power and decode information from the same received signal was considered in [11] and [12]. However, the assumption of simultaneous information decoding and energy harvesting from the same received signal used in [11] and [12] was found to be unrealistic as noted in [13]. It was found in [13] that practical circuits used for harvesting energy from the RF signals are not able to directly decode the information carried by the signal. This is due to the different functionality of the antennas used by the information transceiver and energy harvester in addition to the considerably different power sensitivities of receivers, i.e. -20 to -10 dBm for energy harvesting and -60 dBm for information decoding. This led to the design of two practical receiver architectures,

(a)

(b)
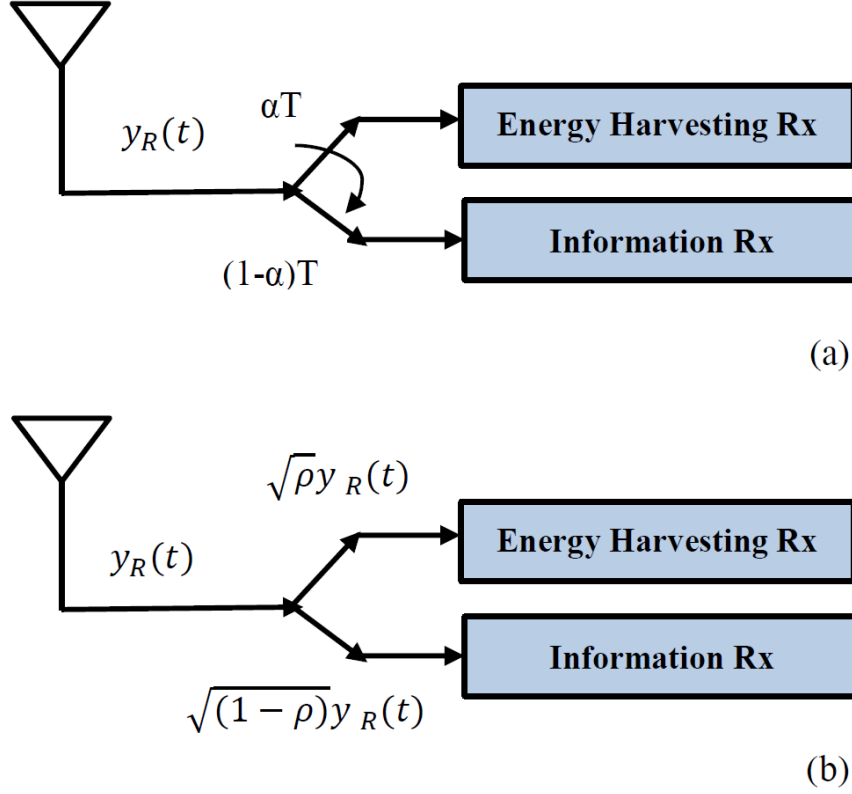
Figure 1.1: (a) TS receiver architecture (b) PS receiver architecture

namely the Time Switching (TS) and the Power Splitting (PS) receiver architectures as shown in Fig. 1.1.

The TS receiver alternately switches between harvesting energy and decoding information. The received RF signal $y_R(t)$ is first sent to the energy harvesting receiver for an amount of time αT, and then to the information receiver for an amount of time $(1 - \alpha)T$, where T is the time duration in which the information signal is transmitted from the source node to the destination node. In the PS receiver the power of the incoming signal is split into two streams by what is called the PS ratio, i.e. ρ. A portion, $\sqrt{\rho}y_R(t)$, of the received signal is sent to the energy harvesting receiver and the remaining portion, $\sqrt{(1 - \rho)}y_R(t)$, of the signal drives the information receiver. Such receivers have been widely adopted in the

4

literature [14],[15],[19]. Based on those designs, Time Switching Relaying (TSR) and Power Splitting Relaying (PSR) protocols have been proposed in [19] for RF energy harvesting in cooperative relay networks.

One of the main challenges facing the wireless energy transfer technology is the high propagation loss. It is shown in [16] that the RF energy transfer distance ranges from 3 to 15 meters for mobile devices depending on the strength of the radiated power, which varies from 1 to 100 Watts. Therefore, RF energy harvesting is only sufficient for powering wireless sensor nodes with low power requirements. Powering devices with larger power requirements has to be performed using additional special stations, called power beacons, which are mainly dedicated for RF energy transfer to mobile devices [17]. Another important challenge is the safety issue, since it has been reported that the exposure limit to microwave radiation, in the 2.4 and 5.8 GHz frequency bands, averaged over 30 minutes is equal to 10 W/m^2 according to the international safety standards [18]. However, this can be mitigated by using phase arrays with smart beamforming techniques, which can ensure the safety in wireless energy transfer using dedicated RF sources [16].

1.3 Resource Allocation in Wireless Networks

Energy sharing has emerged as a promising research area in energy harvesting wireless systems, where the wireless network nodes share their energy resources to enhance the energy efficiency of the network. However, finding the most efficient strategy to utilize the harvested energy to satisfy user requirements, has become a challenging problem for researchers. Various objectives for wireless communication systems have been studied in the literature resulting in different energy allocation strategies. Those objectives include, lifetime maximization, throughput maximization, outage probability minimization, energy efficiency maximization, to-

tal transmit power minimization, transmission time minimization and total energy consumption minimization [30]-[36]. The target objective depends on the studied application and the performance measure under consideration.

For the work on power allocation in wireless cooperative energy harvesting systems done in this thesis, it is assumed that only statistical Channel State Information (CSI) is available at a central managing node. This assumption may be more realistic for energy-constrained networks than assuming full channel CSI availability which requires significant amount of CSI feedback. For a system with a large number of users, it is more practical to consider distributed resource allocation schemes [31]. Those schemes achieve a reasonable tradeoff between the performance measure under consideration and the system complexity, which is a challenging task and is out of the scope of this thesis.

1.4 Organization of the Thesis

The structure of the thesis is as follows

- In Chapter 2, we consider a DF Wireless Relay Network (WRN) consisting of a source node, destination node and an energy-constrained relay node in the presence of an interfering signal. The relay node is capable of RF energy harvesting. For simplicity, we neglect the effect of the RF energy harvested from the interfering signal and study the case where the relay harvests RF energy from the source node. The RF signal sent by the source node carries information which is forwarded via the relay to a destination. We study the performance of three relaying protocols, the TSR protocol, the PSR protocol and a proposed hybrid TSR-PSR protocol. Analytical expressions for the outage probability and throughput in the delay-sensitive transmission mode are derived for the three protocols. A comparison of the throughput performances

of these protocols for different system parameter values is then presented.

- In Chapter 3, we extend our study in Chapter 2 to include the case where the energy-constrained relay node harvests energy from the RF signal sent by the source node in addition to the RF signal of the interferer node. We derive closed-form expressions for the outage probability as well as upper and lower bounds for the considered energy-constrained relay network. We also derive closed-form expressions for the achievable throughputs in the delay-sensitive transmission mode, for the TSR, PSR and the hybrid TSR-PSR protocols. Finally, we present results to illustrate the effect of harvesting energy from the interference signal on the system performance.

- In Chapter 4, various power allocation schemes to distribute the relay's power are studied for a DF WRN consisting of multiple source-destination pairs and one DF relay. The source-destination pairs communicate via the energy-constrained relay which harvests wireless energy from the RF signals transmitted by the source nodes. First a non-shared power allocation scheme is studied in which the RF energy harvested from the i-th source is used to forward information from the relay to the i-th destination. Several shared power allocation schemes are also studied: (1) an equal power allocation scheme, (2) a relay-destination channel dependent scheme, (3) a scheme which maximizes the minimum rate of all relay-destination links, and (4) a scheme which maximizes a weighted-sum-rate of all relay-destination links. Expressions for the outage probability and the throughput in the delay-sensitive transmission mode are derived for each power allocation scheme. The performances of the different allocation schemes are compared in terms of outage probability, throughput and fairness.

- Chapter 5 provides the main findings of the thesis and discusses some possible future research directions.

Chapter 2

RF Energy Harvesting in a Decode-and-Forward Wireless Relay Network

In this chapter we study wireless energy harvesting in a DF WRN in the presence of an interfering signal. The relay node is energy-constrained and harvests energy from the RF signal of the source node. We state the motivation of our work followed by our main contributions. The system model is then presented and analytical expressions for the outage probability and throughput in the delay-sensitive transmission mode are derived for three different relaying protocols. Numerical results are finally presented to compare between the performance of the studied relaying protocols.

2.1   Motivation

Cooperative relaying where intermediate relays assist a source node with the transmission of information to its intended destination is commonly used to improve the energy efficiency of wireless communication systems. However, the relays may be energy-constrained, i.e. no fixed power supply at the relay. Hence, wireless energy harvesting has been studied as a promising solution to prolong the lifetimes of energy-constrained cooperative relay networks [19]-[26]. Based on the commonly

used energy harvesting receiver architectures discussed previously, TSR and PSR protocols have been proposed in [19] for RF energy harvesting in cooperative relay networks.

In [20], the throughput of an AF Two-Way Relay Network (TWRN) with an energy-constrained relay node is derived. Multiple Access Broadcast (MABC) protocol and Time Division Broadcast (TDBC) protocol are considered as two-way relaying protocols. Also three wireless power transfer policies are proposed, namely Dual-Source (DS) power transfer, Single-Fixed-Source (SFS) power transfer and Single-Best-Source (SBS) power transfer, based on the TS receiver architecture. However, interference is not considered when deriving the throughput in [20]. The ergodic capacity of a DF relay network is studied in [21], in which the energy-constrained relay harvests energy from both the received information signal as well as the Co-channel Interference (CCI) signals using the TSR protocol. The achievable throughput is determined based on the derived expression for the ergodic capacity assuming delay-tolerant transmission. A scenario in which multiple source-destination pairs communicate with the help of energy-constrained relays is studied in [22]. This study is focused on the optimal design of SWIPT in relay interference channels. A profile of PS ratios for all relays is derived using game theory, where each link is modeled as a strategic player whose aim is to maximize its individual achievable rate by choosing the relay's PS ratio. The sum-rate of all links is considered as the network-wide performance metric in [22].

In [23], optimal dynamic power splitting policies for the PSR protocol at the energy-constrained relay are studied, to minimize the outage probability of an AF relay network when full CSI and partial CSI are available. The policy with full CSI is found to achieve the best performance but extra system overhead is incurred for channel estimation which is considered to be perfect in this study. In [24], a source

forwards information to a destination via multiple energy-constrained relays in a DF relay network. Two relay selection schemes are discussed depending on the CSI availability, and their outage performances are studied. It is found that there is a tradeoff between the number of relays in the system and the energy harvesting efficiency of the relays. However, no TS or PS is performed in [24] as it is assumed that only one function can be performed in a given time slot. Wireless energy harvesting in a cognitive relay network is studied in [25], where the secondary relay and the secondary source harvest RF energy from the primary signal using the TSR protocol. The interference constraints on the primary and secondary networks are considered in [25] and the outage probability is derived. However, the effect of varying the TS ratio on the outage performance was not studied.

2.2 Contributions

In this chapter, we study wireless energy harvesting and information processing in a DF WRN. The relay is energy-constrained and harvests energy from the source transmissions. The network is subject to interference which affects the system performance. We consider TSR and PSR protocols in [6] for RF energy harvesting at the relay node and we also propose a hybrid TSR-PSR protocol. The outage probabilities and the throughputs of the three protocols are analyzed in the delay-sensitive transmission mode.

The main contributions of this chapter are summarized as follows:

- We propose a hybrid TSR-PSR protocol which enables wireless energy harvesting and information processing at the energy-constrained relay node, based on a combination of the TS and PS receiver architectures.

- We derive closed-form expressions for the outage probability as well as upper

and lower bounds. We also derive closed-form expressions for the achievable throughputs in the delay-sensitive transmission mode of the energy-constrained relay network, for the TSR, PSR and the hybrid TSR-PSR protocols.

• We compare the throughput performances of the three protocols for different system parameters. We show that the throughput of the hybrid protocol is generally higher than those of TSR and PSR.

The remainder of the chapter is organized as follows. In section 2.3, we present our system model. In Sections 2.4, 2.5 and 2.6, we derive the outage probability and the achievable throughput for the TSR, PSR and hybrid protocols, respectively. Numerical results and discussion are presented in section 2.7, followed by a summary in section 2.8.

2.3   System Model

As shown in Fig. 2.1, we consider a DF cooperative relay network, in which the information is transmitted by a source node **S** to a destination node **D** through an energy-constrained relay node **R**. There is no direct link between the source node and the destination node so that the relay assists the transmission of the source information to the destination. The relay harvests energy from the source which transmits at a fixed power P_s. The relay then uses the harvested energy to transmit the information to the destination. We adopt the harvest-use approach in which the harvested energy cannot be stored beyond the current time slot, due to hardware limitation [26]. Moreover, the power required at the relay for information processing is assumed to be negligible compared to the power required for signal transmission from the relay to the destination [13].

The channel gain coefficients from the source to the relay and from the relay
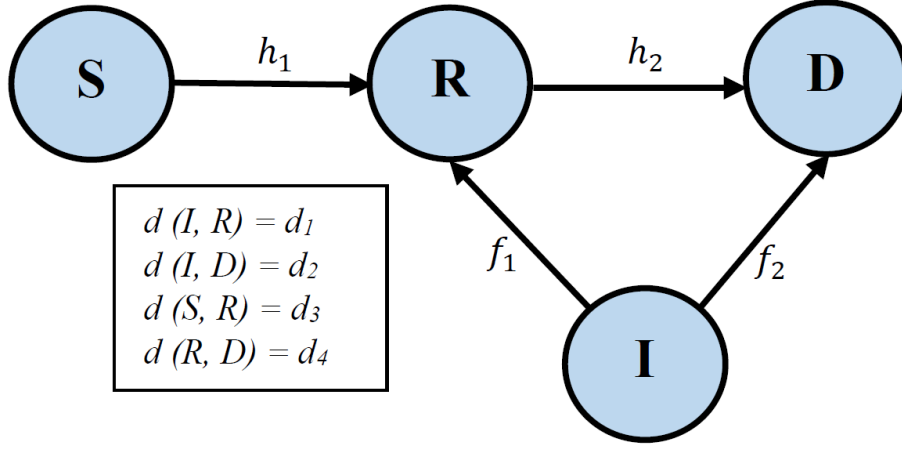
Figure 2.1: System Model

to the destination node are denoted by h_1 and h_2, respectively. We consider an interfering transmitter **I** located at distances d_1 and d_2 from the relay and the destination nodes, respectively, while the corresponding channel gains are denoted by f_1 and f_2. We assume that the interference power is not large enough for RF energy harvesting at the relay. The inter-node distances $\mathbf{S} \to \mathbf{R}$ and $\mathbf{R} \to \mathbf{D}$ are denoted by d_3 and d_4, respectively. We neglect the effect of noise in our system model as the interference power is assumed to be much higher than the noise power. The interference powers received at the relay and the destination are given as [25]

$$P_{\mathcal{I},R} = \frac{P_{\mathcal{I}}|f_1|^2}{d_1^m}, \tag{2.1}$$

$$P_{\mathcal{I},D} = \frac{P_{\mathcal{I}}|f_2|^2}{d_2^m}, \tag{2.2}$$

respectively, where $P_{\mathcal{I}}$ is the interferer transmit power, and m is the path loss exponent.

All links are assumed to be Rayleigh block fading, i.e. the channel is constant over a time slot T, and independent and identically distributed from one slot to

another. Hence $|h_1|^2$, $|h_2|^2$, $|f_1|^2$ and $|f_2|^2$ are exponentially distributed random variables (rvs) with parameters λ_1, λ_2, ν_1 and ν_2 respectively. We consider the TS and PS receiver architectures with PSR and TSR protocols as well as a proposed hybrid TSR-PSR protocol, for the task of energy harvesting and information decoding at the relay node. In the following sections, we derive expressions for the outage probability of each of the relaying protocols as well as the achievable throughputs for the delay-sensitive transmission mode.

2.4 TSR-based Energy Harvesting

The transmission slot structure for the TSR protocol for information decoding and energy harvesting at the relay node is illustrated in Fig. 2.2.

Energy Harvesting at R	S → R Information decoding	R → D Information transmission
αT	$(1-\alpha)T/2$	$(1-\alpha)T/2$
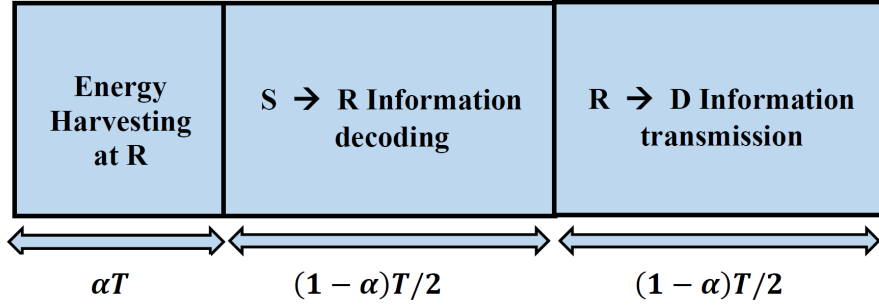
Figure 2.2: TSR protocol at the relay

The slot duration is denoted by T, and α is the fraction of that duration used by the relay for RF energy harvesting from the received source signal. The remaining time $(1-\alpha)T$ is used as follows: $(1-\alpha)T/2$ is used for source to relay communication, and $(1-\alpha)T/2$ is used for relay to destination communication. The energy harvested by the relay and its transmit power are given by

$$E_{h_r} = \frac{\eta P_s |h_1|^2}{d_3^m} \alpha T, \tag{2.3}$$

$$P_r = \frac{E_{h_r}}{(1-\alpha)T/2} = \frac{2\eta P_s |h_1|^2 \alpha}{d_3^m (1-\alpha)}, \tag{2.4}$$

respectively, where $0 < \eta < 1$ is the energy conversion efficiency and P_s is the source power. For notational simplicity, we will replace $|h_1|^2$, $|h_2|^2$, $|f_1|^2$ and $|f_2|^2$ with X_1, X_2, Z_1 and Z_2, respectively. Then the SIRs at the relay and the destination are given respectively as

$$\Gamma_R = \frac{P_s |h_1|^2 d_1^m}{d_3^m P_{\mathcal{I}} |f_1|^2} = \frac{P_s X_1 \beta_{1,3}}{P_{\mathcal{I}} Z_1} = \frac{\rho_R X_1}{Z_1}, \tag{2.5}$$

$$\Gamma_D = \frac{P_r |h_2|^2 d_2^m}{d_4^m P_{\mathcal{I}} |f_2|^2} = \frac{2\eta P_s \alpha X_1 X_2 \beta_{2,4}}{d_3^m (1-\alpha) P_{\mathcal{I}} Z_2} = \frac{\rho_D X_1 X_2}{Z_2}, \tag{2.6}$$

where $\frac{d_1^m}{d_3^m}$ and $\frac{d_2^m}{d_4^m}$ are replaced by $\beta_{1,3}$ and $\beta_{2,4}$ respectively, and $\frac{P_s \beta_{1,3}}{P_{\mathcal{I}}}$ and $\frac{2\eta P_s \alpha \beta_{2,4}}{d_3^m (1-\alpha) P_{\mathcal{I}}}$ are replaced by ρ_R and ρ_D respectively.

2.4.1 Outage Probability

The outage probability is defined as the probability that the Signal to Interference Ratio (SIR) is below a predefined threshold (γ_{th}). The DF relay network is considered to be in outage if either the $\mathbf{S} \rightarrow \mathbf{R}$ link or the $\mathbf{R} \rightarrow \mathbf{D}$ link suffers an outage. In other words, the SIR at the relay or at the destination is smaller than γ_{th}. Note that Γ_R and Γ_D in (2.5) and (2.6) respectively, are statistically dependent since they are both functions of X_1. The outage probability is given as

$$P_{out} = 1 - Pr\left\{ \Gamma_R \geq \gamma_{th}, \Gamma_D \geq \gamma_{th} \right\}. \tag{2.7}$$

Conditioning the outage probability expression on X_1, we can express P_{out} as

$$P_{out} = 1 - \int_0^\infty Pr\left\{ \Gamma_R \geq \gamma_{th} | X_1 = x_1 \right\} \times Pr\left\{ \Gamma_D \geq \gamma_{th} | X_1 = x_1 \right\} f_{X_1}(x_1) dx_1. \tag{2.8}$$

Letting,

$$
\begin{aligned}
\mathcal{J}_1 &= Pr\left\{\Gamma_R \geq \gamma_{th} | X_1 = x_1\right\} = Pr\left\{\frac{\rho_R x_1}{Z_1} \geq \gamma_{th}\right\} \\
&= Pr\left\{Z_1 \leq \frac{\rho_R x_1}{\gamma_{th}}\right\} = 1 - e^{-\frac{\rho_R x_1}{\gamma_{th}\nu_1}},
\end{aligned}
\tag{2.9}
$$

and,

$$
\begin{aligned}
\mathcal{J}_2 &= Pr\left\{\Gamma_D \geq \gamma_{th} | X_1 = x_1\right\} \\
&= Pr\left\{\frac{\rho_D x_1 X_2}{Z_2} \geq \gamma_{th}\right\} = Pr\left\{X_2 \geq \frac{Z_2 \gamma_{th}}{\rho_D x_1}\right\}.
\end{aligned}
\tag{2.10}
$$

Conditioning $\mathcal{J}_2$ in (2.10) on Z_2 and taking the expected value of the results over the distribution of Z_2, we have

$$
\mathcal{J}_2 = \frac{1}{\nu_2} \int_0^\infty e^{-\frac{z_2 \gamma_{th}}{\rho_D x_1 \lambda_2}} e^{-\frac{z_2}{\nu_2}} dz_2 = \frac{\rho_D x_1 \lambda_2}{\gamma_{th}\nu_2 + \rho_D x_1 \lambda_2}
\tag{2.11}
$$

therefore we can write P_{out} as

$$
\begin{aligned}
P_{out} &= 1 - \frac{1}{\lambda_1} \int_0^\infty \left(\mathcal{J}_1 \times \mathcal{J}_2\right) e^{-\frac{x_1}{\lambda_1}} dx_1 \\
&= 1 - \frac{1}{\lambda_1} \int_0^\infty \frac{\rho_D x_1 \lambda_2}{\gamma_{th}\nu_2 + \rho_D x_1 \lambda_2} \left(1 - e^{-\frac{\rho_R x_1}{\gamma_{th}\nu_1}}\right) e^{-\frac{x_1}{\lambda_1}} dx_1 \\
&= 1 - \frac{1}{\lambda_1} \int_0^\infty \frac{x_1}{x_1 + c} \left(1 - e^{-dx_1}\right) e^{-\frac{x_1}{\lambda_1}} dx_1
\end{aligned}
\tag{2.12}
$$

where $c = \frac{\gamma_{th}\nu_2}{\rho_D \lambda_2}$ and $d = \frac{\rho_R}{\gamma_{th}\nu_1}$. The integral in (2.12) can be solved as follows [27]

$$
\int_0^\infty \frac{x}{x+c} e^{-ax} dx = ce^{ca} Ei\left(-ca\right) + \frac{1}{a}
$$

where $Ei\left(x\right) = -\int_{-x}^{\infty}\frac{e^{-t}}{t}dt$ is the exponential integral function. Thus,

$$
\begin{aligned}
P_{out} &= 1 - \frac{1}{\lambda_1}\left(ce^{\frac{c}{\lambda_1}}Ei\left(\frac{-c}{\lambda_1}\right) + \lambda_1 - ce^{cE}Ei\left(-cE\right) - \frac{1}{E}\right) \\
&= -\frac{c}{\lambda_1}e^{\frac{c}{\lambda_1}}Ei\left(\frac{-c}{\lambda_1}\right) + \frac{c}{\lambda_1}e^{cE}Ei\left(-cE\right) + \frac{1}{\lambda_1 E},
\end{aligned}
\tag{2.13}
$$

where $E = d + 1/\lambda_1$. Given that $E_1\left(x\right) = -Ei\left(-x\right)$, then P_{out} can be rewritten as

$$
P_{out} = \frac{c}{\lambda_1}e^{\frac{c}{\lambda_1}}E_1\left(\frac{c}{\lambda_1}\right) - \frac{c}{\lambda_1}e^{cE}E_1\left(cE\right) + \frac{1}{\lambda_1 E}
\tag{2.14}
$$

The exponential integral function, $E_1(x)$, can be upper and lower bounded by [28]:

$$
\frac{1}{2}e^{-x}\ln(1 + \frac{2}{x}) < E_1(x) < e^{-x}\ln(1 + \frac{1}{x}),
\tag{2.15}
$$

thus we have the following upper and lower bounds on P_{out}:

$$
\begin{aligned}
P_{out-upper} &= \frac{c}{\lambda_1}\ln\left(1 + \frac{\lambda_1}{c}\right) - \frac{c}{\lambda_1}\ln\left(1 + \frac{1}{cE}\right) + \frac{1}{\lambda_1 E}, \tag{2.16} \\
P_{out-lower} &= \frac{c}{2\lambda_1}\ln\left(1 + \frac{2\lambda_1}{c}\right) - \frac{c}{2\lambda_1}\ln\left(1 + \frac{2}{cE}\right) + \frac{1}{\lambda_1 E}. \tag{2.17}
\end{aligned}
$$

2.4.2 Throughput

The achievable throughput for the delay-sensitive transmission mode is defined as the throughput achieved such that the destination node has to decode the received signal in its time slot. In this mode, the throughput in units of bit/s/Hz, is defined as the maximum constant rate R_{ds}, where $R_{ds} = \log_2(1 + \gamma_{th})$, that can be maintained over fading blocks with a specified outage probability, i.e. the throughput is given by [19]

$$
\tau_{ds} = \frac{\frac{(1-\alpha)T}{2}}{T}R_{ds}(1 - P_{out}) = \frac{1-\alpha}{2}R_{ds}(1 - P_{out}).
\tag{2.18}
$$

2.5   PSR-based Energy Harvesting

When the PS receiver is implemented at the relay, a fraction ρ, i.e. power-split ratio, of the source power P_s is used for energy harvesting while the remaining power, i.e. $(1 - \rho)P_s$, is used for information decoding, as shown in Fig. 2.3.
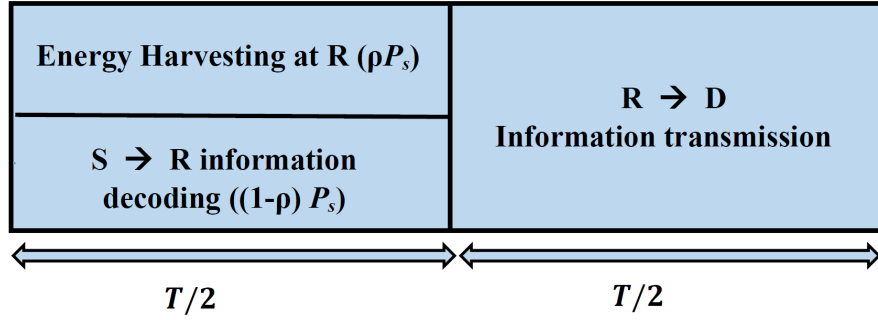
Figure 2.3: PSR protocol at the relay

Thus, the energy harvested at the relay and its transmit power are given by

$$E_{h_r} = \frac{\eta \rho P_s |h_1|^2}{d_3^m} \times \frac{T}{2}, \tag{2.19}$$

$$P_r = \frac{E_{h_r}}{T/2} = \frac{\eta \rho P_s X_1}{d_3^m}. \tag{2.20}$$

The portion of the received signal used for information decoding can be expressed as

$$y_R = \sqrt{\frac{(1 - \rho)P_s}{d_3^m}} h_1 x_s, \tag{2.21}$$

where x_s is the signal transmitted from the source node.

2.5.1   Outage Probability

The SIRs at the relay and the destination can be expressed respectively as

$$\Gamma_R = \frac{P_s(1 - \rho)|h_1|^2 d_1^m}{d_3^m P_{\mathcal{I}} |f_1|^2} = \frac{P_s(1 - \rho)X_1 \beta_{1,3}}{P_{\mathcal{I}} Z_1} = \rho_{R_2} \frac{X_1}{Z_1}, \tag{2.22}$$

18

$$\Gamma_D = \frac{P_r|h_2|^2 d_2^m}{d_4^m P_{\mathcal{I}}|f_2|^2} = \frac{\eta\rho P_s X_1 X_2 \beta_{2,4}}{d_3^m P_{\mathcal{I}} Z_2} = \rho_{D_2}\frac{X_1 X_2}{Z_2}. \tag{2.23}$$

The outage probability is defined as in (2.7) and following a similar derivation as in Subsection 2.4.1, the outage probability can be expressed as

$$P_{out} = \frac{c_2}{\lambda_1}e^{\frac{c_2}{\lambda_1}}E_1\left(\frac{c_2}{\lambda_1}\right) - \frac{c_2}{\lambda_1}e^{c_2 E_2}E_1\left(c_2 E_2\right) + \frac{1}{\lambda_1 E_2}. \tag{2.24}$$

Using the upper and lower bounds for the exponential integral in (2.15), we obtain expressions similar to $P_{out-upper}$ in (2.16) and $P_{out-lower}$ in (2.17) as follows

$$P_{out-upper} = \frac{c_2}{\lambda_1}\ln\left(1+\frac{\lambda_1}{c_2}\right) - \frac{c_2}{\lambda_1}\ln\left(1+\frac{1}{c_2 E_2}\right) + \frac{1}{\lambda_1 E_2}, \tag{2.25}$$

$$P_{out-lower} = \frac{c_2}{2\lambda_1}\ln\left(1+\frac{2\lambda_1}{c_2}\right) - \frac{c_2}{2\lambda_1}\ln\left(1+\frac{2}{c_2 E_2}\right) + \frac{1}{\lambda_1 E_2}, \tag{2.26}$$

where c is replaced by $c_2 = \frac{\gamma_{th}\nu_2}{\rho_{D_2}\lambda_2}$, and E is replaced by $E_2 = \frac{\rho_{R_2}}{\gamma_{th}\nu_1} + \frac{1}{\lambda_1}$.

2.5.2 Throughput

Similar to our previous derivation in Subsection 2.4.2, we evaluate the throughput for the delay-sensitive transmission mode. For the PS receiver, we have

$$\tau_{ds} = \frac{T/2}{T}R_{ds}(1-P_{out}) = \frac{1}{2}R_{ds}(1-P_{out}). \tag{2.27}$$

By comparing the throughput expressions in (2.18) and (2.27) for TSR and PSR respectively, we can observe that the throughput in PSR is generally higher than that in TSR given that the outage probabilities for PSR and TSR are quite similar. This can be further explained by the fact that the PSR protocol uses $T/2$ for source to relay communication and the remaining $T/2$ for relay to destination communication. Two functions are performed within the first $T/2$ block which are harvesting RF

energy from the source signal as well as source to relay information transmission. In the second $T/2$ block, the relay to destination information transmission takes place. On the other hand the TSR uses a dedicated fraction of time αT just for RF energy harvesting from the source transmissions. Then the remaining portion of time is divided into two halves, the first half is for source to relay information transmission, and the other half is for relay to destination information transmission. Therefore the overall amount of time for information transmission in the TSR protocol is usually lesser than that in the PSR, which may generally lead to a lower throughput.

2.6 Hybrid TSR-PSR-based Energy Harvesting

In this section, we consider a hybrid TS and PS receiver architecture which results in a generalized version of PSR and TSR as shown in Fig. 2.4. The PSR protocol
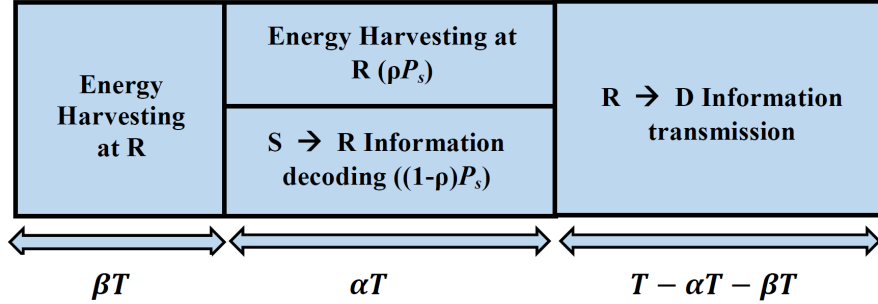
Figure 2.4: Hybrid TSR-PSR protocol at the relay

is a special case of this hybrid protocol when $\beta = 0$ and $\alpha = 0.5$, while the TSR protocol is a special case when $\rho = 0$ and $\alpha = \frac{1-\beta}{2}$. The portion of time βT is used for energy harvesting from the source power P_s. The source signal is divided into two streams during the portion of time αT. During this time a fraction of the power ρP_s is used for energy harvesting from the source signal by the relay node, and a fraction $(1-\rho)P_s$ is used for decoding the information signal at the relay node. The

remaining $T - \alpha T - \beta T$ is the portion of time used for information transmission between the relay and the destination node.

2.6.1 Outage Probability

The energy harvested by the relay and the relay transmit power are given by

$$
\begin{aligned}
E_{h_r} &= \frac{\eta P_s X_1}{d_3^m}\beta T + \frac{\eta \rho P_s X_1}{d_3^m}\alpha T, & (2.28)\\
P_r &= \frac{E_{h_r}}{(1-\alpha-\beta)T} = \frac{\eta P_s X_1 \beta}{d_3^m(1-\alpha-\beta)} + \frac{\eta \rho P_s X_1 \alpha}{d_3^m(1-\alpha-\beta)}. & (2.29)
\end{aligned}
$$

The SIRs at the relay and destination nodes are given by

$$
\begin{aligned}
\Gamma_R &= \frac{P_s(1-\rho)X_1\beta_{1,3}}{P_I Z_1} = \rho_{R_3}\frac{X_1}{Z_1}, & (2.30)\\
\Gamma_D &= \frac{P_r X_2 \beta_{2,4}}{P_I Z_2} = \rho_{D_3}\frac{X_1 X_2}{Z_2}, & (2.31)
\end{aligned}
$$

where $\rho_{D_3} = \frac{\eta P_s \beta_{2,4}}{P_I d_3^m(1-\alpha-\beta)}(\beta + \rho\alpha)$. Using (2.7), we can derive the outage probability for the hybrid protocol as

$$
P_{out} = \frac{c_3}{\lambda_1}e^{\frac{c_3}{\lambda_1}}E_1\left(\frac{c_3}{\lambda_1}\right) - \frac{c_3}{\lambda_1}e^{c_3 E_3}E_1\left(c_3 E_3\right) + \frac{1}{\lambda_1 E_3}, \qquad (2.32)
$$

where $c_3 = \frac{\nu_2 \gamma_{th}}{\rho_{D_3}\lambda_2}$ and $E_3 = \frac{\rho_{R_3}}{\gamma_{th}\nu_1} + \frac{1}{\lambda_1}$.

2.6.2 Throughput

Following the analysis in Subsection 2.4.2, the throughput for the proposed hybrid TSR-PSR in the delay-sensitive transmission mode can be obtained as

$$
\tau_{ds} = (1-\alpha-\beta)R_{ds}(1-P_{out}). \qquad (2.33)
$$

It was found in the cases we studied that $\beta = 0$ provided the best throughput. This follows our previous explanation of the superiority of the PSR over the TSR protocol, which is due to using a dedicated portion of time only for energy harvesting in the TSR, thus leading to a decrease in the overall information transmission time. In this case (2.33) reduces to

$$\tau_{ds} = (1 - \alpha)R_{ds}(1 - P_{out}). \tag{2.34}$$

Note that when $\beta = 0$, the hybrid protocol in Fig. 2.4 becomes a generalized version of the PSR protocol in Fig. 2.3 with a factor α (instead of $\frac{1}{2}$ used in the conventional PSR protocol), which denotes the fraction of time used for source to relay communication. The remaining fraction, i.e. $(1 - \alpha)$, is then used for relay to destination communication. The proposed hybrid protocol can perform better than the PSR protocol if the parameters α and ρ are well chosen. This can be explained since the $\mathbf{S} - \mathbf{R}$ and the $\mathbf{R} - \mathbf{D}$ link gains are generally different, and thus it may be better to assign more time to the channel with the poorer channel condition.

2.7 Numerical Results

In this section we present numerical results to validate the outage probability and throughput expressions derived for the proposed relay-assisted network with RF energy harvesting. We examine the outage probability and the throughput expressions as a function of α and ρ, moreover we show the throughput as a function of P_s, $P_\mathcal{I}$, d_3 and d_4. We assume that the source, relay, and destination nodes are located at (0, 0), (1, 0), and (2, 0) on the X-Y plane respectively, while the interferer node is located at (1.5, 2). The energy harvesting efficiency η is set to 1, the path loss exponent $m = 4$, the SIR threshold value $\gamma_{th} = 0$ dB, and the means of all the

channel gain coefficients λ_1, λ_2, ν_1 and ν_2 are equal to 5. The simulation results were obtained over 10^6 Rayleigh channel realizations.
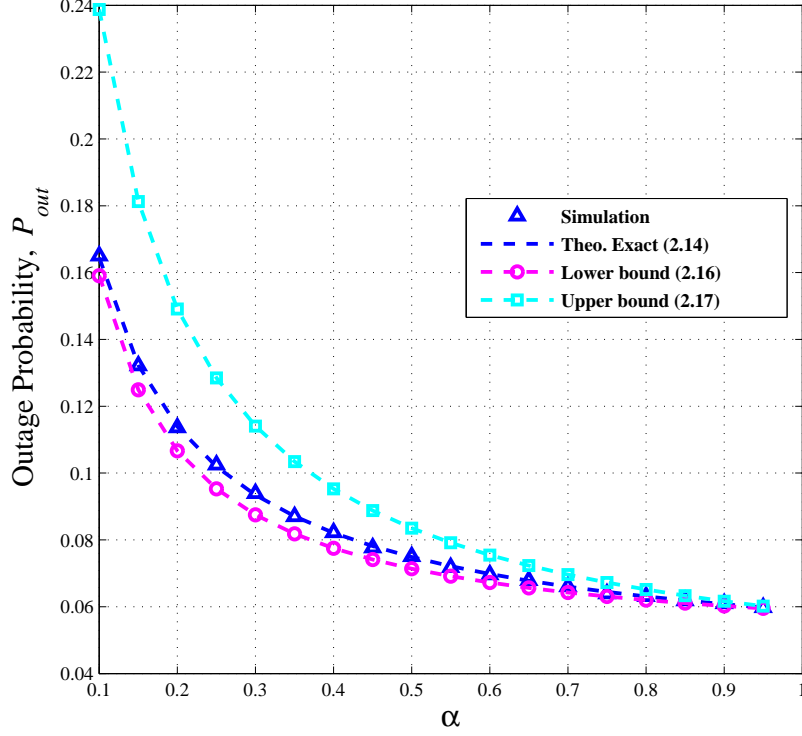
Figure 2.5: Outage probability versus α for the TSR protocol

Fig. 2.5 shows the outage probability in (2.14) for the TSR protocol, the upper and lower bounds in (2.16) and (2.17) respectively, as well as the simulation results. Fig. 2.6 shows the outage probability in (2.24) for the PSR protocol, as well as the upper and lower bounds. It can be seen from Figs. 2.5 and 2.6 that there is good agreement between the simulation and the analytical results. In addition to that, both figures show that the lower bound for the outage probability gives a better approximation than the upper bound. Moreover Fig. 2.6 shows that there is an optimal PS value, i.e. ρ, which results in the minimum outage probability.
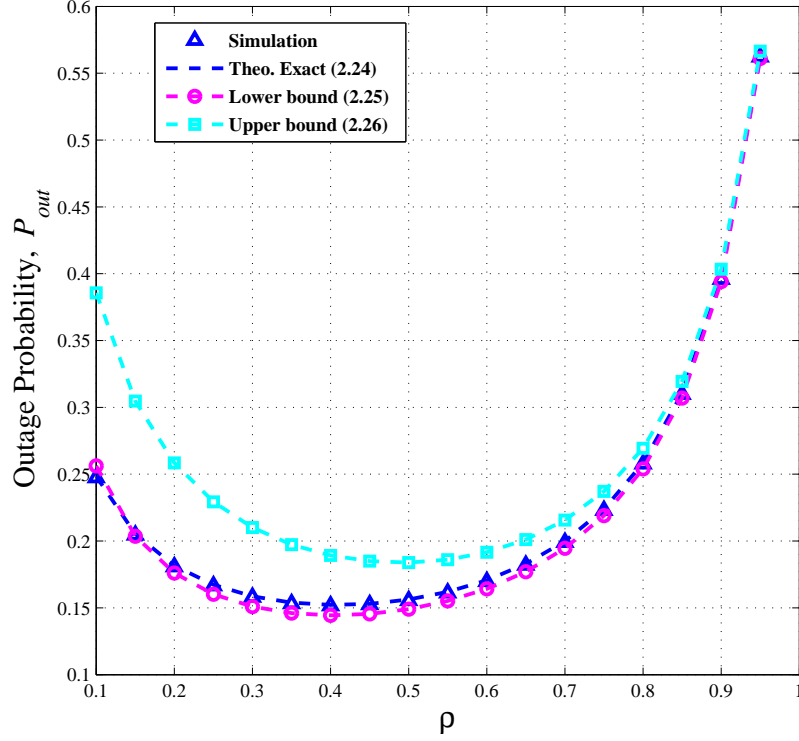
Figure 2.6: Outage probability versus ρ for the PSR protocol

The outage probability results for the hybrid protocol are shown in Fig. 2.7, where we plot P_{out} as a function of α for different values of ρ. It can be observed from Fig. 2.7 that the outage probability decreases as α increases. On the other hand, $0.3 \leq \rho \leq 0.7$ generally gives the best outage probability performance as shown in the figure. Note that the TS ratio, i.e. α, should not be increased to its maximum possible value since there is a tradeoff between the outage probability and the throughput of the hybrid and the TSR protocols, which mainly depends on the choice of the parameter α, as illustrated in Fig. 2.8.
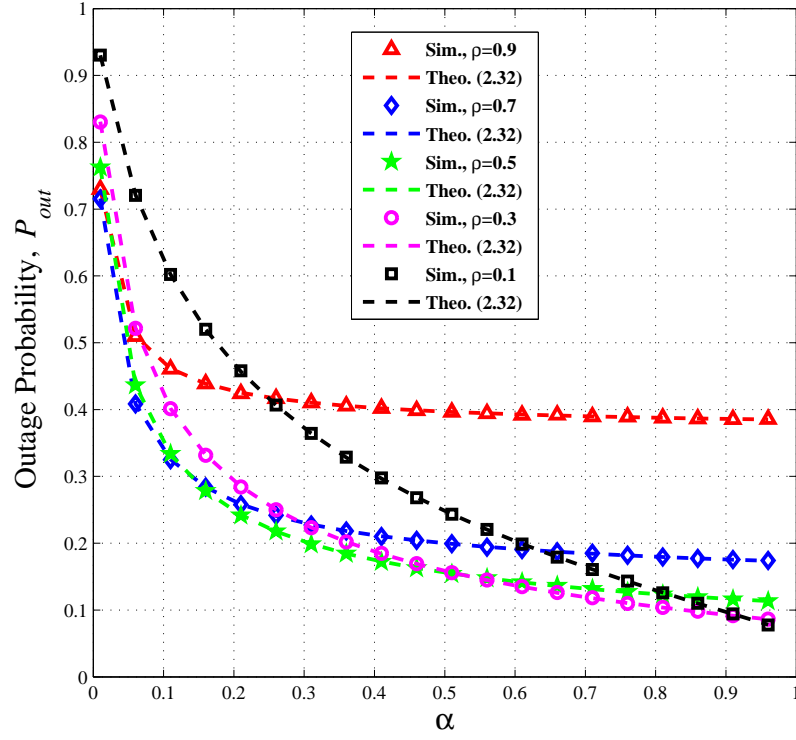
Figure 2.7: Outage probability versus α for the hybrid protocol with various ρ values
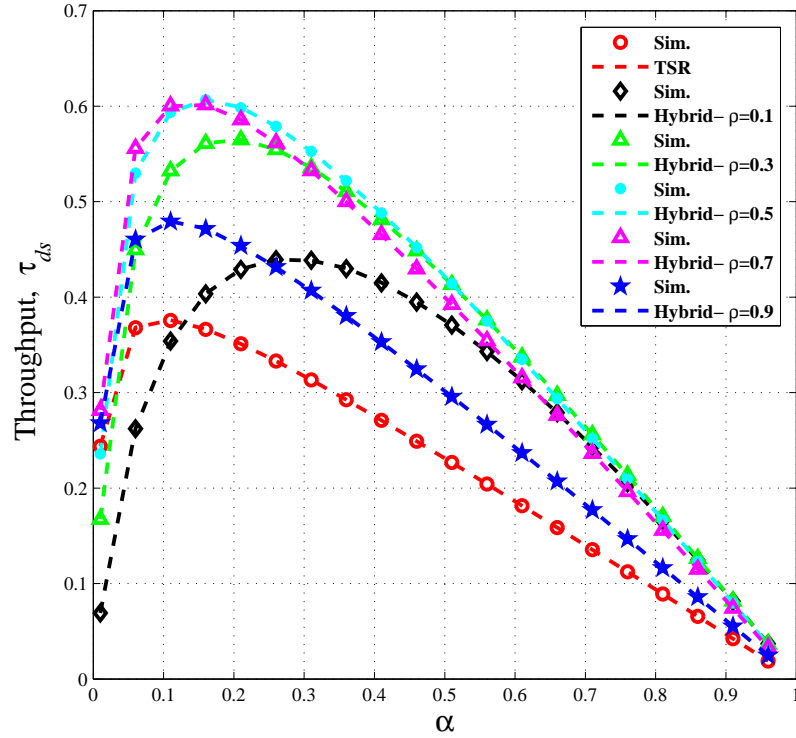
Figure 2.8: Throughput versus α for the hybrid and the TSR protocols

Fig. 2.8 shows the throughput as a function of α, i.e. the TS ratio, for the TSR protocol as well as the hybrid protocol for various fixed ρ values, i.e. the PS ratio. It can be observed that the hybrid protocol outperforms the TSR protocol with well-chosen TS and PS parameters. It can be seen from the figure that the best throughput performance of the hybrid protocol can be achieved with PS ratios in the range, $0.3 \leq \rho \leq 0.7$, and the TS ratios in the range, $0.1 \leq \alpha \leq 0.3$. This was similarly observed in Fig. 2.7 which showed that the best outage probability of the hybrid protocol was obtained for the same range of the PS ratios as in Fig. 2.8.
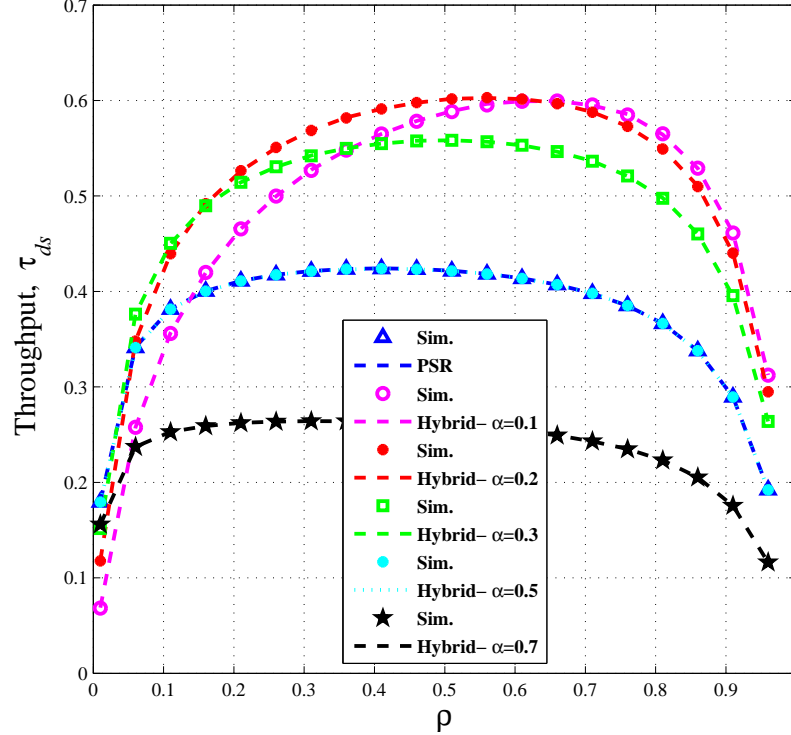
Figure 2.9: Throughput versus ρ for the hybrid and the PSR protocols

Fig. 2.9 shows the throughput as a function of ρ, i.e. the PS ratio, for the PSR protocol as well as the hybrid protocol for various fixed α values, i.e. the TS

ratio. As expected when $\alpha = \frac{1}{2}$ the throughput of the hybrid protocol coincides with that of the PSR protocol since they become the same. Moreover it is observed from the figure that the hybrid protocol outperforms the PSR protocol when the parameters α and ρ are properly chosen. The best throughput performance of the hybrid protocol can be achieved with a TS ratio in the range, $0.1 \leq \alpha \leq 0.3$, for a wide range of the chosen PS ratio.

Figure 2.10: Throughput versus P_s for TSR, PSR and the hybrid protocol

Fig. 2.10 shows the throughput as a function of P_s for the three protocols. It can be seen that as P_s increases, the throughput increases for all protocols. This is expected since an increase in the source power will lead to an increase in the energy harvested by the relay. The PSR outperforms the TSR, as explained previously and

by observing their expressions in (2.27) and (2.18) respectively. We also observe that the hybrid protocol outperforms both the TSR and the PSR protocols depending on the choice of the TS and PS ratios. In Fig. 2.10 the hybrid protocol gives the best throughput performance for $\alpha = 0.2$ and $\rho = 0.6$.
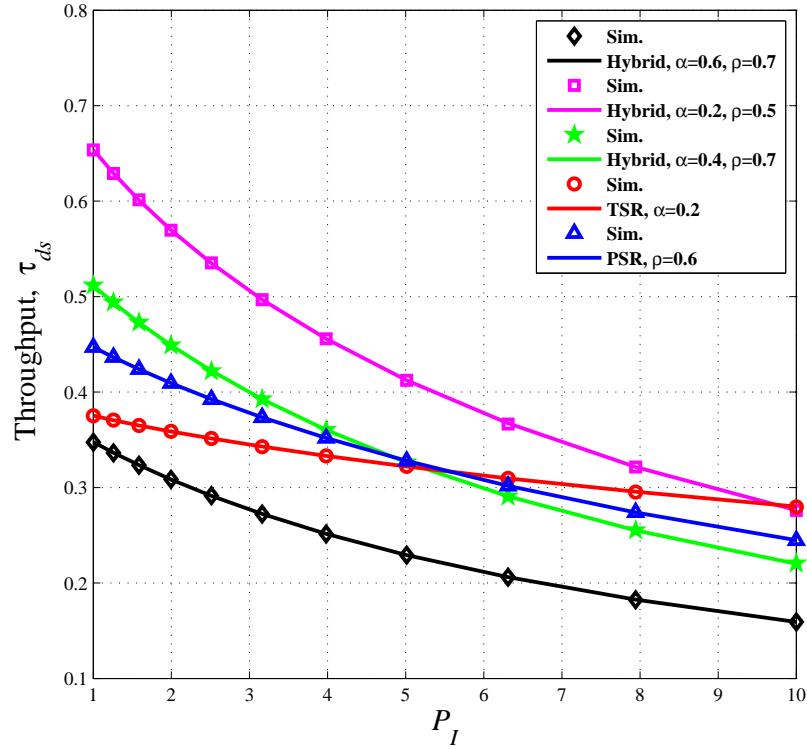
Figure 2.11: Throughput versus $P_{\mathcal{I}}$ for TSR, PSR and the hybrid protocol

Fig. 2.11 shows the throughput as a function of $P_{\mathcal{I}}$ for the three protocols. As to be expected, the throughput decreases as $P_{\mathcal{I}}$ increases since the SIR decreases leading to an increase in the outage probability. We note that for high values of $P_{\mathcal{I}}$, i.e. low SIR values, the throughput of the TSR protocol becomes slightly better than that of the PSR, which was previously observed in [19] for low signal-to-noise-ratios (SNRs). Furthermore we note that the hybrid protocol gives the best throughput

performance for well-chosen values of α and ρ (e.g. $\alpha = 0.2, \rho = 0.5$).
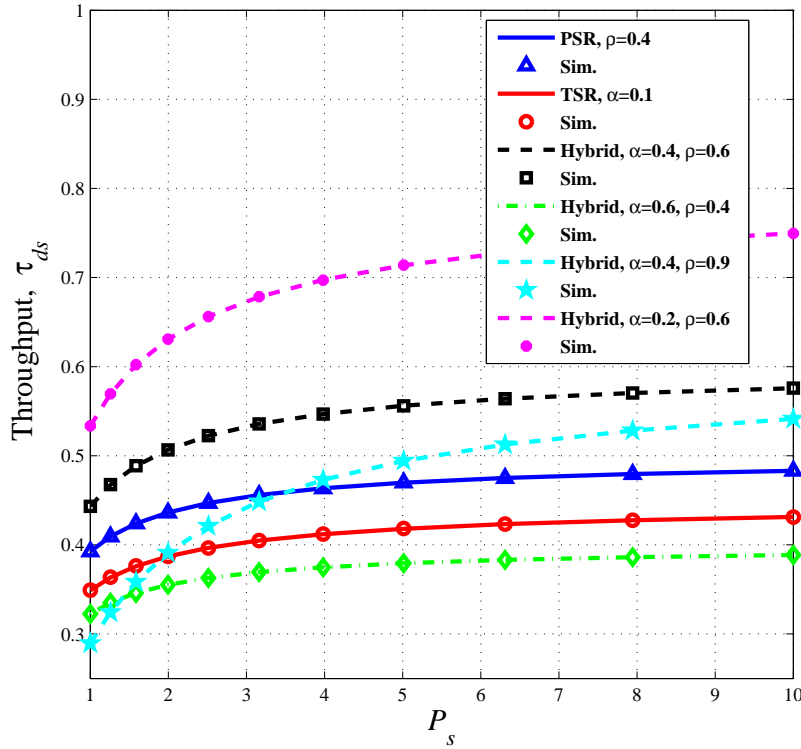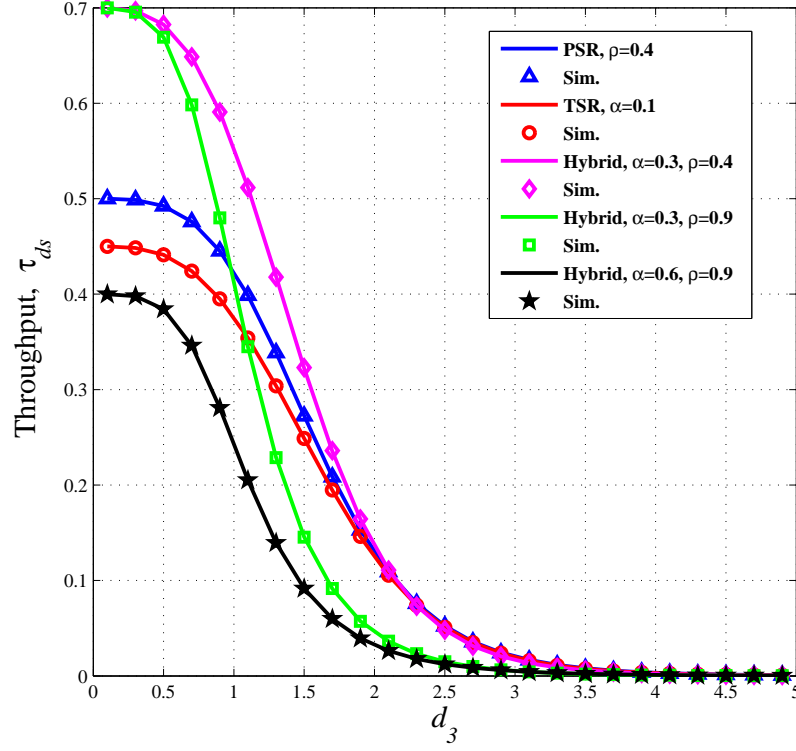

Figure 2.12: Throughput versus d_3 for TSR, PSR and the hybrid protocol

Fig. 2.12 shows the throughput as a function of d_3 which is the distance between the source and relay nodes. As expected, the throughput decreases as d_3 increases. The hybrid protocol gives the best throughput performance for $\alpha = 0.3, \rho = 0.4$.

On the other hand Fig. 2.13 shows the throughput as a function of d_4 which is the distance between the relay and destination nodes. It can be observed that the throughput decreases as d_4 increases which is expected and similarly observed in the previous figure. The hybrid protocol gives the best throughput performance for $\alpha = 0.3$ and $0.5 \leq \rho \leq 0.7$, while the PSR outperforms the TSR protocol as observed in all the figures presented so far.
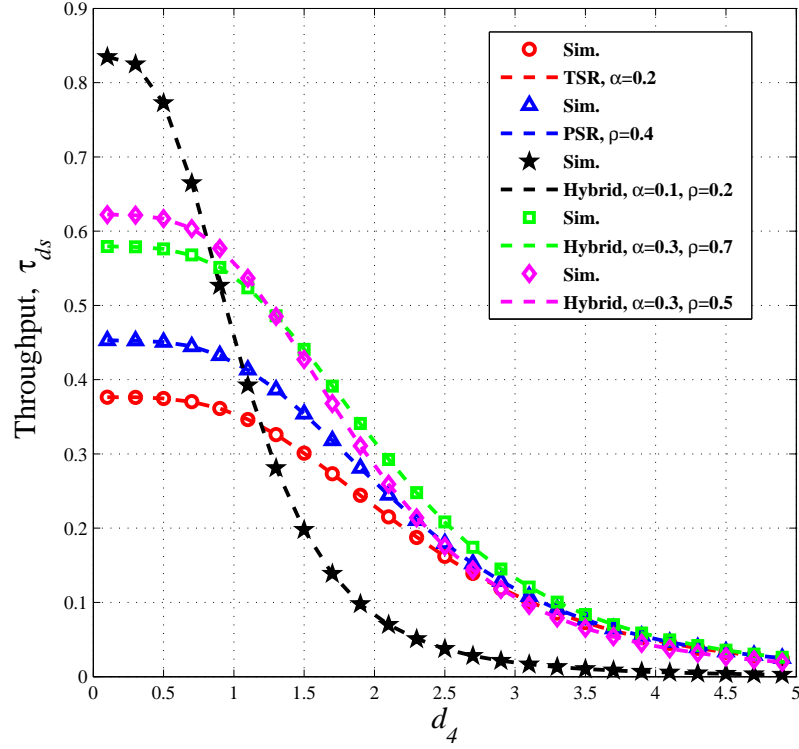
Figure 2.13: Throughput versus d_4 for TSR, PSR and the hybrid protocol

2.8 Summary

Three wireless energy harvesting protocols for DF relay networks in presence of interference were studied. Analytical expressions for the outage probability and the throughput in the delay-sensitive transmission mode were derived and validated using computer simulations. Numerical results were used to show the effect of various system parameters on the throughput of the studied protocols. The results demonstrate that the proposed hybrid protocol generally yields a better throughput performance than the TSR and PSR protocols given that the TS and PS ratios are chosen properly.

Chapter 3

RF Energy Harvesting from Interference Signals in a DF Wireless Relay Network

In Chapter 2, we studied the outage probability and the throughput of a WRN with an energy-constrained relay harvesting RF energy from the source transmissions in the presence of interference. In this chapter we study the case when the relay harvests RF energy from both the source transmissions as well as the interference. We derive the outage probability and the throughput and compare the results with those obtained in Chapter 2 to examine the effect of harvesting energy from interference on the system performance.

3.1 Motivation and Contributions

In the previous chapter, we studied the case when the RF energy that the relay can harvest from the interference signal is assumed to be negligible. In this chapter we study the more general case when this assumption is dropped. The outage probability and throughput derivations in this general case are somewhat more complex than those obtained in Chapter 2. We then study the effect of harvesting energy from the interference on the system performance, given the same system configuration

assumed in Chapter 2. The contributions of this chapter are as follows:

- We derive closed-form expressions for the outage probability, as well as upper and lower bounds, for the considered energy-constrained relay network. We also derive closed-form expressions for the achievable throughputs in the delay-sensitive transmission mode, for the TSR, PSR and the hybrid TSR-PSR protocols. The derived expressions are generalized versions of the expressions obtained in Chapter 2.

- We compare the throughput performance of each of the TSR, PSR and the hybrid protocols, with and without RF energy harvesting from the interference assuming the same system parameters as in Chapter 2. We examine the improvement achieved to test the validity of neglecting the energy harvested from the interference signal.

The remainder of this chapter is organized as follows. Section 3.2 describes our system model. The system outage probability and the throughput in the delay-sensitive transmission mode are derived in Sections 3.3, 3.4 and 3.5, for the TSR, PSR and hybrid protocols, respectively. Numerical results are presented in Section 3.6, followed by a summary in Section 3.7.

3.2 System Model

Our system model is similar to that studied in Chapter 2, Fig. 2.1. The only difference is that we include the effect of RF energy harvesting from the interference signal in addition to the source signal, instead of the source signal alone as assumed in Chapter 2. Our goal here is to compare the performance in terms of the outage probability and throughput for each of the TSR, PSR and the hybrid protocols with the corresponding achieved performance presented in Chapter 2.

3.3   TSR-based Energy Harvesting

The transmission slot structure is the same as in Fig. 2.2, where the slot duration is denoted by T, and αT is the time used by the relay for RF energy harvesting from the received source signal and the interference signal. The remaining time is divided equally such that $(1-\alpha)T/2$ is used for source to relay communication, and $(1-\alpha)T/2$ is used for relay to destination communication. The energy harvested by the relay and its transmit power are given respectively by

$$E_{h_r} = \left(\frac{\eta P_s X_1}{d_3^m} + \frac{\eta P_{\mathcal{I}} Z_1}{d_1^m}\right)\alpha T, \tag{3.1}$$

$$P_r = \frac{E_{h_r}}{(1-\alpha)T/2} = \frac{2\eta P_s X_1 \alpha}{d_3^m(1-\alpha)} + \frac{2\eta P_{\mathcal{I}} Z_1 \alpha}{d_1^m(1-\alpha)}, \tag{3.2}$$

where $0 < \eta < 1$ is the energy conversion efficiency, P_s is the source power and $P_{\mathcal{I}}$ is the interferer transmit power. The SIRs at the relay and at the destination are

$$\Gamma_R = \frac{P_s X_1 d_1^m}{d_3^m P_{\mathcal{I}} Z_1} = \rho_R \frac{X_1}{Z_1}, \tag{3.3}$$

$$\Gamma_D = \frac{P_r X_2 d_2^m}{d_4^m P_{\mathcal{I}} Z_2} = (a_1 X_1 + b_1 Z_1)\frac{X_2}{Z_2} = \frac{W X_2}{Z_2}, \tag{3.4}$$

where we replace $\frac{d_1^m}{d_3^m}$ and $\frac{d_2^m}{d_4^m}$ by $\beta_{1,3}$ and $\beta_{2,4}$ respectively, thus $a_1 = \frac{2\eta P_s \beta_{2,4}\alpha}{d_3^m(1-\alpha)P_{\mathcal{I}}}$, $b_1 = \frac{2\eta \beta_{2,4}\alpha}{d_1^m(1-\alpha)}$ and $W = a_1 X_1 + b_1 Z_1$.

3.3.1   Outage Probability and Throughput Analysis

The DF relay network is considered to be in outage, if either the SIR at the relay node or that at the destination node is below some predefined threshold γ_{th}, which is given by

$$P_{out} = 1 - Pr\left\{\Gamma_R \ge \gamma_{th}, \Gamma_D \ge \gamma_{th}\right\}. \tag{3.5}$$

From the SIR expressions in (3.3) and (3.4) we observe that they are independent.
The outage probability can thus be expressed as

$$P_{out} \;\; = \;\; 1 - (Pr\,\{\Gamma_R \geq \gamma_{th}\} \times Pr\,\{\Gamma_D \geq \gamma_{th}\}) = 1 - (\mathcal{I}_R \times \mathcal{I}_D). \qquad (3.6)$$

Now we evaluate $\mathcal{I}_R$ and $\mathcal{I}_D$ as follows

$$
\begin{aligned}
\mathcal{I}_R \;\; &= \;\; Pr\left\{\rho_R \frac{X_1}{Z_1} \geq \gamma_{th}\right\} = Pr\left\{X_1 \geq \frac{\gamma_{th} Z_1}{\rho_R}\right\} \\
&= \;\; \frac{1}{\nu_1} \int_0^\infty e^{-\frac{\gamma_{th} z_1}{\rho_R \lambda_1}} \times e^{\frac{-z_1}{\nu_1}}\, dz_1 \\
&= \;\; \frac{1}{\nu_1} \times \left[\frac{e^{-\left(\frac{\gamma_{th}}{\rho_R \lambda_1} + \frac{1}{\nu_1}\right)}}{-\left(\frac{\gamma_{th}}{\rho_R \lambda_1} + \frac{1}{\nu_1}\right)} \right]_0^\infty \\
&= \;\; \frac{\rho_R \lambda_1}{\nu_1 \gamma_{th} + \rho_R \lambda_1}, \qquad (3.7)
\end{aligned}
$$

$$\mathcal{I}_D = \int_0^\infty Pr\,\{\Gamma_D \geq \gamma_{th}|W = w\} \times f_W(w)dw. \qquad (3.8)$$

Now $\mathcal{I}_D|_W$ can be evaluated as

$$
\begin{aligned}
\mathcal{I}_D|_W \;\; &= \;\; Pr\,\{\Gamma_D \geq \gamma_{th}|W = w\} \\
&= \;\; Pr\left\{\frac{w X_2}{Z_2} \geq \gamma_{th}\right\} = Pr\left\{X_2 \geq \frac{\gamma_{th} Z_2}{w}\right\} \\
&= \;\; \frac{1}{\nu_2} \int_0^\infty e^{-\frac{\gamma_{th} z_2}{w \lambda_2}} \times e^{-\frac{z_2}{\nu_2}}\, dz_2 \\
&= \;\; \frac{1}{\nu_2} \times \left[\frac{e^{-\left(\frac{\gamma_{th}}{w \lambda_2} + \frac{1}{\nu_2}\right)}}{-\left(\frac{\gamma_{th}}{w \lambda_2} + \frac{1}{\nu_2}\right)} \right]_0^\infty \\
&= \;\; \frac{w \lambda_2}{\gamma_{th} \nu_2 + w \lambda_2} = \frac{w}{w + c}, \qquad (3.9)
\end{aligned}
$$

where $c = \frac{\gamma_{th} \nu_2}{\lambda_2}$.

To find an expression for $\mathcal{I}_D$ in (3.8) we need the probability density function

(pdf) of the rv $W = U + V$, where $U = a_1 X_1$ and $V = b_1 Z_1$. Since a_1 and b_1 are constants, X_1 and Z_1 are exponentially distributed independent Random Variable (rv)s, then U and V are exponentially distributed independent rvs as well with means $a_1 \lambda_1$ and $b_1 \nu_1$ respectively, and pdfs

$$
f_U(u) = \frac{1}{a_1 \lambda_1} e^{-\frac{u}{a_1 \lambda_1}}, \tag{3.10}
$$

$$
f_V(v) = \frac{1}{b_1 \nu_1} e^{-\frac{v}{b_1 \nu_1}}. \tag{3.11}
$$

Therefore the sum $W = U + V$ is a rv with a density function $f_W(w)$, given by the convolution of f_U and f_V [29]

$$
\begin{aligned}
f_W(w) &= \int_{-\infty}^{\infty} f_U(w-x) \times f_V(x) dx = \int_0^w f_U(w-x) \times f_V(x) dx, W \geq 0 \\
&= \frac{1}{a_1 \lambda_1} \times \frac{1}{b_1 \nu_1} \int_0^w e^{-\left(\frac{w-x}{a_1 \lambda_1}\right)} \times e^{-\left(\frac{x}{b_1 \nu_1}\right)} dx \\
&= \frac{e^{\frac{-w}{a_1 \lambda_1}}}{a_1 \lambda_1 b_1 \nu_1} \int_0^w e^{-x\left(\frac{1}{b_1 \nu_1} - \frac{1}{a_1 \lambda_1}\right)} dx \\
&= \frac{e^{\frac{-w}{a_1 \lambda_1}}}{a_1 \lambda_1 b_1 \nu_1} \times \left[\frac{-e^{-x\left(\frac{1}{b_1 \nu_1} - \frac{1}{a_1 \lambda_1}\right)}}{\frac{1}{b_1 \nu_1} - \frac{1}{a_1 \lambda_1}} \right]_0^w \\
&= \frac{1}{a_1 \lambda_1 - b_1 \nu_1} \times \left(e^{\frac{-w}{a_1 \lambda_1}} - e^{\frac{-w}{b_1 \nu_1}} \right). \tag{3.12}
\end{aligned}
$$

Substituting (3.12) into (3.8) yields

$$
\mathcal{I}_D = \frac{1}{a_1 \lambda_1 - b_1 \nu_1} \times \int_0^{\infty} \frac{w}{w+c} \times \left(e^{\frac{-w}{a_1 \lambda_1}} - e^{\frac{-w}{b_1 \nu_1}} \right) dw. \tag{3.13}
$$

The expression in (3.13) can be written in terms of the exponential integral function

$E_1(.)$ [27] as

$$\mathcal{I}_D = \frac{1}{a_1\lambda_1 - b_1\nu_1} \times \left[-ce^{\frac{c}{a_1\lambda_1}} E_1\left(\frac{c}{a_1\lambda_1}\right) + a_1\lambda_1 + ce^{\frac{c}{b_1\nu_1}} E_1\left(\frac{c}{b_1\nu_1}\right) - b_1\nu_1 \right].$$
(3.14)

Upper and lower bounds can be obtained as in (2.15) as

$$\mathcal{I}_{D-lower} = \frac{1}{a_1\lambda_1 - b_1\nu_1} \times \left[\frac{-c}{2}\ln\left(1 + \frac{2a_1\lambda_1}{c}\right) + a_1\lambda_1 + \frac{c}{2}\ln\left(1 + \frac{2b_1\nu_1}{c}\right) - b_1\nu_1 \right],$$
(3.15)

$$\mathcal{I}_{D-upper} = \frac{1}{a_1\lambda_1 - b_1\nu_1} \times \left[-c\ln\left(1 + \frac{a_1\lambda_1}{c}\right) + a_1\lambda_1 + c\ln\left(1 + \frac{b_1\nu_1}{c}\right) - b_1\nu_1 \right].$$
(3.16)

Substituting the derived expressions, (3.7) for $\mathcal{I}_R$, and (3.14)-(3.16) for $\mathcal{I}_D, \mathcal{I}_{D-lower}$ and $\mathcal{I}_{D-upper}$ respectively, in (3.6), the outage probability as well as the upper and lower bounds can be obtained as follows

$$P_{out,TSR} = 1 - (\mathcal{I}_R \times \mathcal{I}_D),$$
(3.17)

$$P_{out-upper,TSR} = 1 - (\mathcal{I}_R \times \mathcal{I}_{D-upper}),$$
(3.18)

$$P_{out-lower,TSR} = 1 - (\mathcal{I}_R \times \mathcal{I}_{D-lower}).$$
(3.19)

Following the analysis in Chapter 2, Subsection 2.4.2, the throughput for the TSR protocol in the delay-sensitive transmission mode can be obtained as

$$\tau_{ds,TSR} = \left(\frac{1-\alpha}{2}\right) \times R_{ds}\left(1 - P_{out,TSR}\right).$$
(3.20)

3.4 PSR-based Energy Harvesting

The PSR protocol transmission slot structure is shown in Fig. 2.3. The total slot duration T is divided equally such that half of it is used for source to relay communication while the other half is used for relay to destination communication. The relay harvests a fraction ρ of the source's signal power, while it decodes the information signal using the remaining source power, i.e. $(1 - \rho)P_s$ in the first $\frac{T}{2}$. The energy harvested by the relay and its transmit power are given as follows

$$E_{h_r} = \left(\frac{\eta \rho P_s X_1}{d_3^m} + \frac{\eta \rho P_{\mathcal{I}} Z_1}{d_1^m} \right) \times \frac{T}{2}, \tag{3.21}$$

$$P_r = \frac{E_{h_r}}{T/2} = \frac{\eta \rho P_s X_1}{d_3^m} + \frac{\eta \rho P_{\mathcal{I}} Z_1}{d_1^m}. \tag{3.22}$$

3.4.1 Outage Probability and Throughput Analysis

The SIRs at the relay node and the destination node are given by

$$\Gamma_R = \frac{P_s(1 - \rho)X_1 d_1^m}{d_3^m P_{\mathcal{I}} Z_1} = \rho_{R_2} \frac{X_1}{Z_1}, \tag{3.23}$$

$$\Gamma_D = \frac{P_r X_2 d_2^m}{d_4^m P_{\mathcal{I}} Z_2} = (a_2 X_1 + b_2 Z_1) \frac{X_2}{Z_2} = \frac{W X_2}{Z_2}, \tag{3.24}$$

where $a_2 = \frac{\eta \rho P_s \beta_{2,4}}{d_3^m P_{\mathcal{I}}}$, $b_2 = \frac{\eta \rho \beta_{2,4}}{d_1^m}$, $\rho_{R_2} = \frac{P_s(1 - \rho)d_1^m}{d_3^m P_{\mathcal{I}}}$ and $W = a_2 X_1 + b_2 Z_1$. From (3.23) and (3.24), it can be seen that Γ_R and Γ_D are independent. The outage probability is thus given by (3.6).

Expressions for $\mathcal{I}_R$ and $\mathcal{I}_D$ can be obtained in a way similar to that in Subsection 3.3.1

$$\mathcal{I}_R = Pr \left\{ \rho_{R_2} \frac{X_1}{Z_1} \geq \gamma_{th} \right\} = \frac{\rho_{R_2} \lambda_1}{\nu_1 \gamma_{th} + \rho_{R_2} \lambda_1}, \tag{3.25}$$

$$\mathcal{I}_D = \frac{1}{a_2 \lambda_1 - b_2 \nu_1} \times \left[-ce^{\frac{c}{a_2 \lambda_1}} E_1 \left(\frac{c}{a_2 \lambda_1} \right) + a_2 \lambda_1 + ce^{\frac{c}{b_2 \nu_1}} E_1 \left(\frac{c}{b_2 \nu_1} \right) - b_2 \nu_1 \right], \tag{3.26}$$

where $c = \frac{\gamma_{th}\nu_2}{\lambda_2}$. Upper and lower bounds for $\mathcal{I}_D$ are similar to (3.15) and (3.16) respectively, where a_1 and b_1 are replaced by a_2 and b_2. Substituting (3.25) and (3.26) in (3.6), we obtain the outage probability, i.e. $P_{out,PSR}$, for the PSR protocol. The throughput for the PSR protocol in the delay-sensitive transmission mode is obtained using the $P_{out,PSR}$ expression as follows

$$\tau_{ds,PSR} = \frac{1}{2} \times R_{ds}\left(1 - P_{out,PSR}\right). \tag{3.27}$$

3.5 Hybrid TSR-PSR-based Energy Harvesting

In this section we consider the transmission slot structure in Fig. 3.1 which is the same as the one in Fig. 2.4 with $\beta = 0$. The hybrid slot structure is a generalized version of the PSR protocol in which the total slot duration T is not divided equally, but rather by a fraction α. The fraction α, denotes the time used for source to relay communication, which constitutes energy harvesting and information transmission. The remaining fraction, i.e. $(1 - \alpha)$, is used for relay to destination communication.
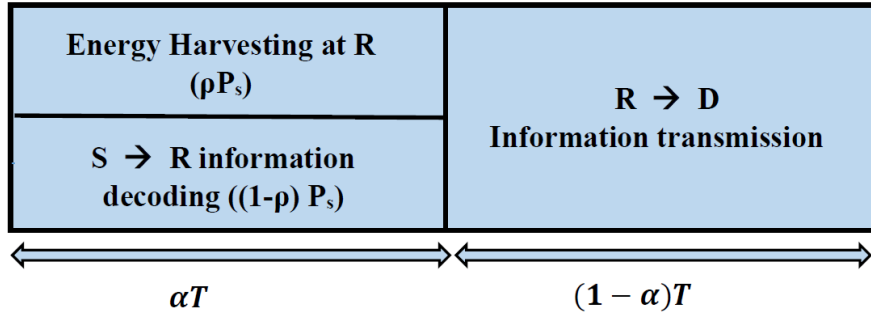

Figure 3.1: Hybrid TSR-PSR protocol at the relay

The energy harvested by the relay and its transmit power are given by

$$E_{h_r} = \left(\frac{\eta \rho P_s X_1}{d_3^m} + \frac{\eta \rho P_{\mathcal{I}} Z_1}{d_1^m} \right) \times \alpha T, \tag{3.28}$$

$$P_r = \frac{E_{h_r}}{(1-\alpha)T} = \frac{\eta \rho \alpha P_s X_1}{d_3^m (1-\alpha)} + \frac{\eta \rho P_{\mathcal{I}} Z_1}{d_1^m (1-\alpha)}, \tag{3.29}$$

where α and ρ should be chosen carefully in order to adjust the throughput performance of the hybrid protocol as shown in Chapter 2.

3.5.1 Outage Probability and Throughput Analysis

The SIRs at the relay node and the destination node for the hybrid protocol are

$$\Gamma_R = \frac{P_s(1-\rho)X_1 d_1^m}{d_3^m P_{\mathcal{I}} Z_1} = \rho_{R_2} \frac{X_1}{Z_1}, \tag{3.30}$$

$$\Gamma_D = \frac{P_r X_2 d_2^m}{d_4^m P_{\mathcal{I}} Z_2} = (a_3 X_1 + b_3 Z_1) \frac{X_2}{Z_2} = \frac{W X_2}{Z_2}, \tag{3.31}$$

where $a_3 = \frac{\eta \rho \alpha P_s \beta_{2,4}}{d_3^m (1-\alpha) P_{\mathcal{I}}}$, $b_3 = \frac{\eta \rho \alpha \beta_{2,4}}{d_1^m (1-\alpha)}$ and $W = a_3 X_1 + b_3 Z_1$. Note that Γ_R in (3.30) and Γ_D in (3.31) are independent. The outage probability, i.e. $P_{out,hybrid}$, for the hybrid protocol can thus be obtained by finding expressions for $\mathcal{I}_R$ and $\mathcal{I}_D$, and substituting them in (3.6), as done in Subsection 3.3.1. From (3.30), it can be seen that Γ_R for the hybrid protocol is equal to that for PSR protocol in (3.23), thus the expression for $\mathcal{I}_R$ is equal to that in (3.25). The expression for $\mathcal{I}_D$ can be obtained as

$$\mathcal{I}_D = \frac{1}{a_3 \lambda_1 - b_3 \nu_1} \times \left[-ce^{\frac{c}{a_3 \lambda_1}} E_1 \left(\frac{c}{a_3 \lambda_1} \right) + a_3 \lambda_1 + ce^{\frac{c}{b_3 \nu_1}} E_1 \left(\frac{c}{b_3 \nu_1} \right) - b_3 \nu_1 \right]. \tag{3.32}$$

Upper and lower bounds for $\mathcal{I}_D$ are similar to (3.15) and (3.16) respectively, by replacing a_1 and b_1 by a_3 and b_3 respectively. Finally the throughput of the hybrid

protocol in the delay-sensitive transmission mode can be obtained as

$$\tau_{ds,hybrid} = (1 - \alpha) \times R_{ds} \left(1 - P_{out,hybrid}\right).$$ (3.33)

3.6   Numerical Results

In this section we present numerical results to validate the outage probability, throughput expressions and the upper and lower bounds derived for the WRN discussed, considering RF energy harvesting from the information as well as the interference signals. We compare the performance achieved when harvesting energy from the interference and information signals versus harvesting energy from the information signal alone, a case which was studied in Chapter 2. The system configuration is the same as in Chapter 2: the source, relay, destination and interferer nodes are located at $(0, 0)$, $(1, 0)$, $(2, 0)$ and $(1.5, 2)$ on the X-Y plane respectively. The energy harvesting efficiency $\eta = 1$, the path loss exponent $m = 4$, the SIR threshold value $\gamma_{th} = 0$ dB, and the means of all the channel gain coefficients λ_1, λ_2, ν_1 and ν_2 are equal to 5.

Fig. 3.2 shows the outage probability for the TSR protocol in (3.17) versus α, i.e. the TS ratio, as well as the upper and lower bounds in (3.18) and (3.19) respectively, and the simulation results. It can be seen that the lower bound given in (3.18) is closer to the exact outage probability curve than the upper bound in (3.19), which was similarly observed in Chapter 2.

In Fig. 3.3 we plot the throughput of the TSR and the hybrid protocols versus α while the throughput of the PSR protocol is shown versus ρ. We compare the throughput of each when harvesting RF energy from the interference and information signals versus the case when harvesting RF energy from the information signal only. It can be seen that there is a slight increase in the throughput performance
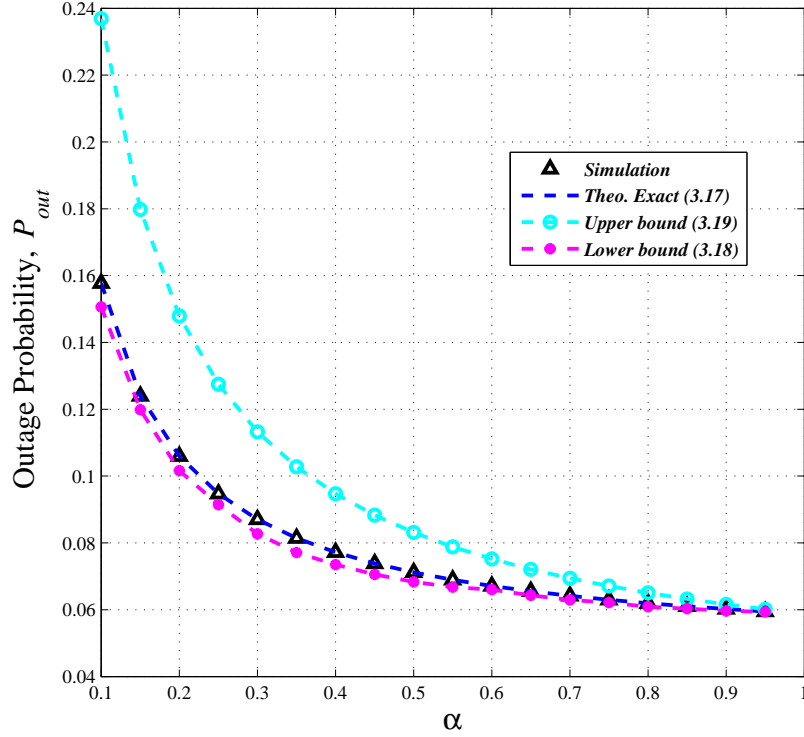
Figure 3.2: Outage Probability versus α for the TSR protocol

when considering RF energy harvesting from the interference. This small improvement can be explained by the fact that both the relay and the destination nodes are subject to interference from the interferer node. Therefore the gain achieved from harvesting the RF energy from the interference signal by the relay node is offset by the decrease in the SIR at the destination node caused by the interference signal.

Fig. 3.4 shows the throughput for the studied relaying protocols versus the interference power $P_{\mathcal{I}}$, with and without harvesting energy from the interference signal. It can be observed that the throughput decreases as $P_{\mathcal{I}}$ increases. There is a slight performance improvement when considering RF energy harvesting from both the interference and information signals. This improvement is more noticeable for the TSR and the hybrid protocols than that for the PSR protocol.
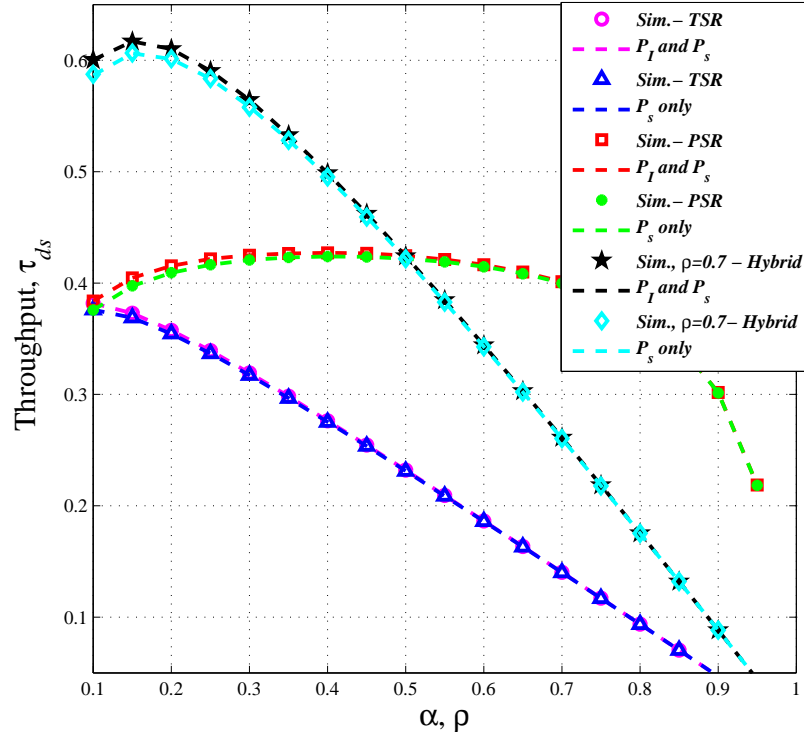
Figure 3.3: Throughput versus α for the TSR and the hybrid protocols and versus ρ for the PSR protocol

42

Figure 3.4: Throughput versus $P_{\mathcal{I}}$ for the TSR, PSR and the hybrid protocols
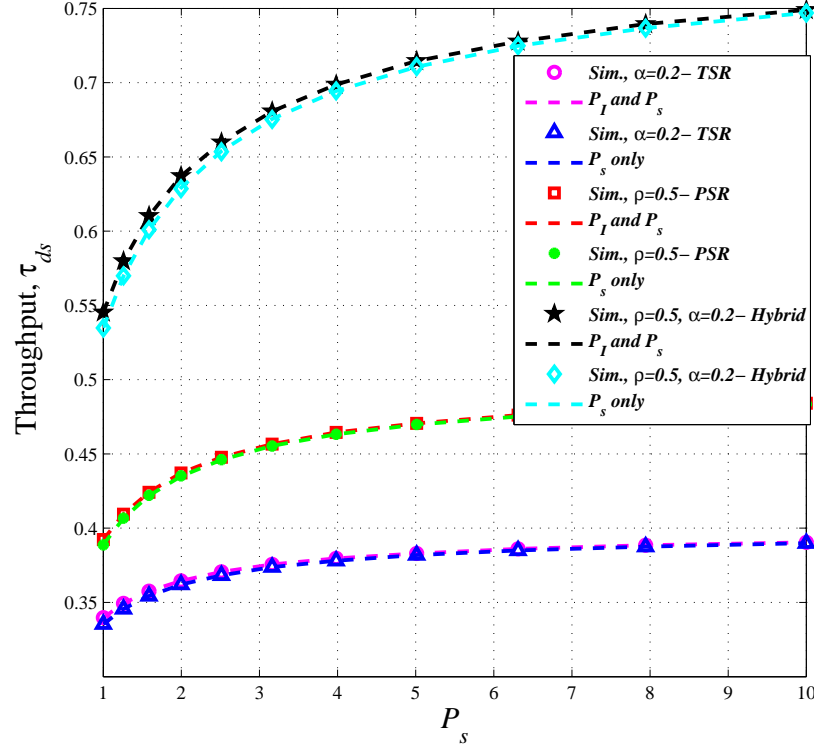
Figure 3.5: Throughput versus P_s for the TSR, PSR and the hybrid protocols

The throughput of each of the studied relaying protocols versus the source power P_s, is shown in Fig. 3.5. It can be observed that the performance improvement for all relaying protocols when harvesting energy from the interference signal is very small compared to that when energy harvesting from the interference signal is not considered.

In Figs. 3.6 and 3.7 we show the throughput of each of the studied relaying protocols versus the $\mathbf{S} - \mathbf{R}$ internode distance d_3, and the $\mathbf{R} - \mathbf{D}$ internode distance d_4, respectively. From Figs. 3.6 and 3.7, it can be seen that the throughput for each of the relaying protocols are nearly the same with and without harvesting RF energy from the interference.
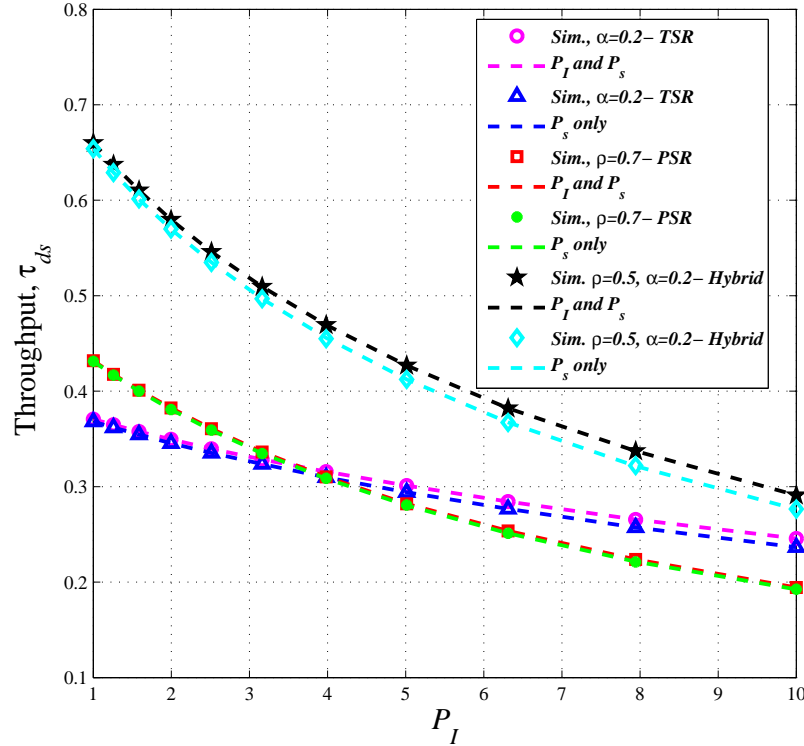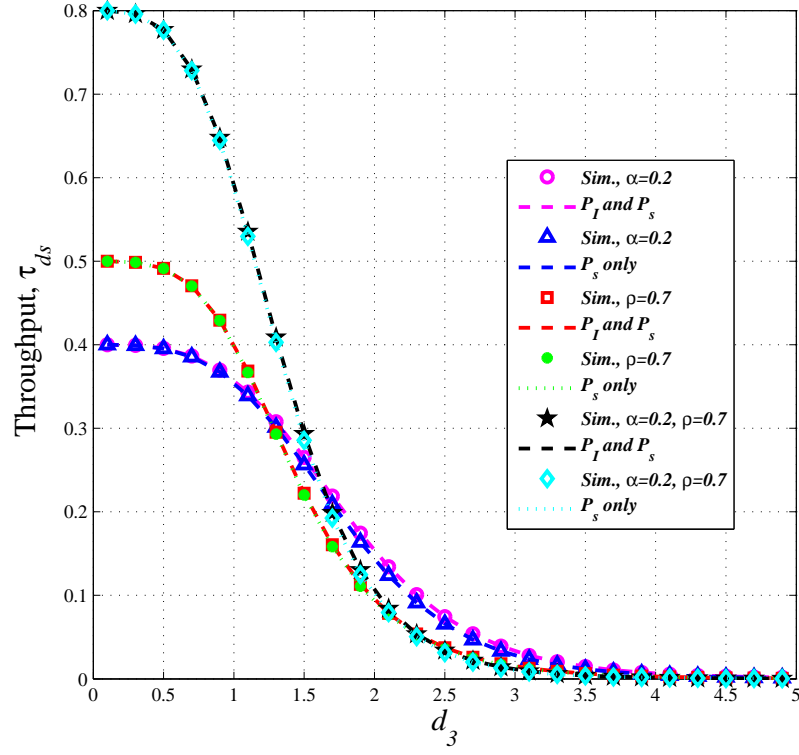
Figure 3.6: Throughput versus d_3 for the TSR, PSR and the hybrid protocols

44
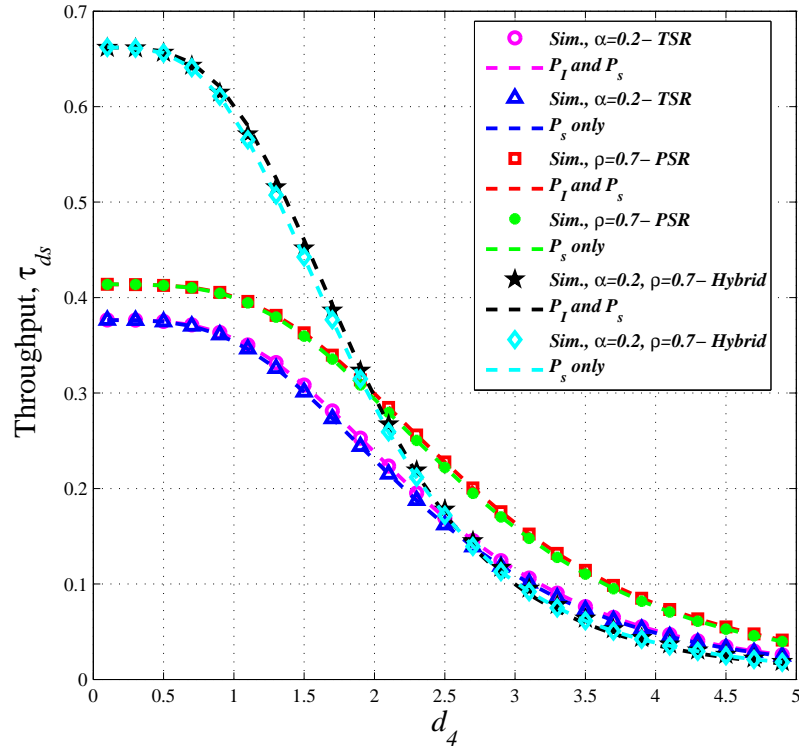
Figure 3.7: Throughput versus d_4 for the TSR, PSR and the hybrid protocols

In summary it can be seen from Figs. 3.3-3.7, that the throughput improvement achieved due to including harvesting energy from the interference signal is very small. This is due to our assumed system configuration which makes the RF energy harvested from the source signal larger than that harvested from the interference signal. The improvement would have been more significant in case the harvested energy from the interference signal was comparable or much larger than that harvested from the source signal.

3.7 Summary

In this chapter we extended the study in Chapter 2, by considering the case where RF energy is harvested from both the interference and information signals. We derive expressions for the outage probability and throughput in the delay-sensitive mode for this general case. Using the same system parameters and configurations as in Chapter 2, we compare the throughput performance with the case studied previously, in which the relay's harvested energy from the interference signal is neglected. Our results show that there is only a slight performance improvement in terms of throughput and outage probability. However, this improvement is insignificant due to our assumed system configuration, which makes the RF energy harvested by the relay from the source signal much larger than that harvested from the interference signal.

Chapter 4

Power Allocation in a DF Wireless Relay Network with RF Energy Harvesting

In this chapter, we study different power allocation schemes for a two-hop DF WRN consisting of multiple source-destination pairs and a single relay harvesting energy from the source transmissions under Rayleigh fading. We state the motivation and contributions, followed by the system model description. First we consider a non-shared power allocation scheme, then four different shared power allocation schemes are studied. All schemes are compared in terms of outage probability, throughput and fairness. Performance evaluation results are provided and finally, a summary is given at the end of this chapter.

4.1 Motivation

Relays are employed in wireless networks to split the path from the source to the destination into shorter hops, in order to improve the energy efficiency of the network and prolong its lifetime. In the previous chapters, we studied the outage probability and the throughput in the delay-sensitive transmission mode of a DF WRN with one source-destination pair. In this chapter, we study the case when we have multiple

source-destination pairs assisted by one energy-constrained relay which harvests RF energy from the source transmissions.

The main problem when having a scenario with multiple source-destination pairs and one relay, is to allocate the relay's power among the different relay-destination links, so as to achieve some desired objective. SWIPT is studied in a cooperative clustered WSN in [30], where energy-constrained relays harvest RF energy from the source node transmissions to prolong its lifetime. The optimal transmission power, relay selection and PS ratio are determined so as to maximize the energy efficiency of the system. In [31] the authors study the power allocation problem in a DF WRN with multiple source-destination pairs and one RF energy harvesting relay. Two centralized allocation schemes based on equal power allocation and sequential waterfilling are studied, as well as an auction-based allocation strategy to realize distributed power allocation. The focus in [31] is to distribute the RF energy harvested by the relay among the different relay-destination links to minimize the outage probability of the system. The study in [32] focused on maximizing the data rate per unit energy in both AF and DF cooperative networks with multiple source-destination pairs and one energy harvesting relay. A closed-form solution for the optimal power allocation scheme is obtained for the non-cooperative case, i.e. when the relay harvests energy and forwards information from the i-th source to the i-th destination. While an energy cooperation scheme is applied at the relay node to find the optimal PS ratio for the cooperative transmission case. The problem in [32] is a non-convex optimization problem, and is solved by proposing an iterative algorithm where the update in each iteration consists of a group of convex problems with a continuous parameter. It is shown in [32] that the solution can have fast convergence to the optimum, and the results show that the proposed algorithm can enhance the system sum rate compared with the non-cooperative scheme. The spatial randomness of

user locations is taken into account in [33] when the outage probability is derived for a cooperative network with multiple source-destination pairs communicating with each other via an energy harvesting relay. Efficient power allocation schemes for multi-user AF WRNs are developed in [34] according to several different objectives: (1) the minimum SNR among all users is maximized, (2) the maximum transmit power over all sources is minimized and (3) the network throughput is maximized. Moreover a joint admission control and power allocation algorithm for the system is proposed. Power allocation schemes to maximize the minimum rate among all users as well as to maximize the weighted-sum of rates have been proposed in [35] for wireless multi-user AF relay networks. A distributed algorithm was also developed using the dual decomposition approach for the problem of maximizing the weighted-sum of rates. The study in [36] considers a multi-user single-relay AF network, and uses game theory to derive the power allocation of the relay power among the users. However, energy harvesting is not considered in [34]-[36].

4.2   Contributions

In this chapter we consider a cooperative DF WRN with multiple source-destination pairs, one energy harvesting relay and one interferer node. Shared and non-shared allocation schemes are studied to allocate the relay's harvested power among different relay-destination transmissions. Our main figures of merit are the outage probability, throughput in the delay-sensitive mode and fairness.

The main contributions of this chapter are summarized as follows:

- The single source-destination pair model studied in Chapter 2 is extended to the multiple source-destination pairs, in which the relay harvests RF energy and forwards information from the i-th source to its corresponding i-th destination.

- An equal power allocation scheme [31] is studied as one of the shared allocation schemes, such that the relay divides the harvested power from all the sources evenly among the relay-destination pairs.

- A power allocation scheme is proposed and studied, in which the relay allocates the minimum power required for the user with the best channel condition first, followed by the user with the second best channel condition if there is any power left at the relay, and so on. If the relay has energy left over after all users have been allocated their minimum required powers, the residual energy is equally divided between relay-destination links.

- Other criteria to distribute the relay's harvested power are examined. First we consider a power allocation which maximizes the minimum rate of all relay-destination links, followed by a weighted-sum-rate maximization of all relay-destination links.

The remainder of this chapter is organized as follows, the system model is presented in Section 4.3. The outage probability and the throughput of the non-shared power allocation scheme as well as of the different shared allocation schemes are analyzed in Sections 4.4 and 4.5 respectively. Numerical results and discussion are presented in Section 4.6, followed by a summary in Section 4.7.

4.3 System Model

We consider a wireless cooperative network with N source-destination pairs denoted as $\mathbf{S}_i - \mathbf{D}_i$, $i = 1, ..., N$, and one energy harvesting relay $\mathbf{R}$ as shown in Fig. 4.1. There is no direct link between the source-destination pairs, so each source communicates with its intended destination via the relay. The cooperative transmission divides the transmission time slot into two halves, each of duration $\frac{T}{2}$. The first
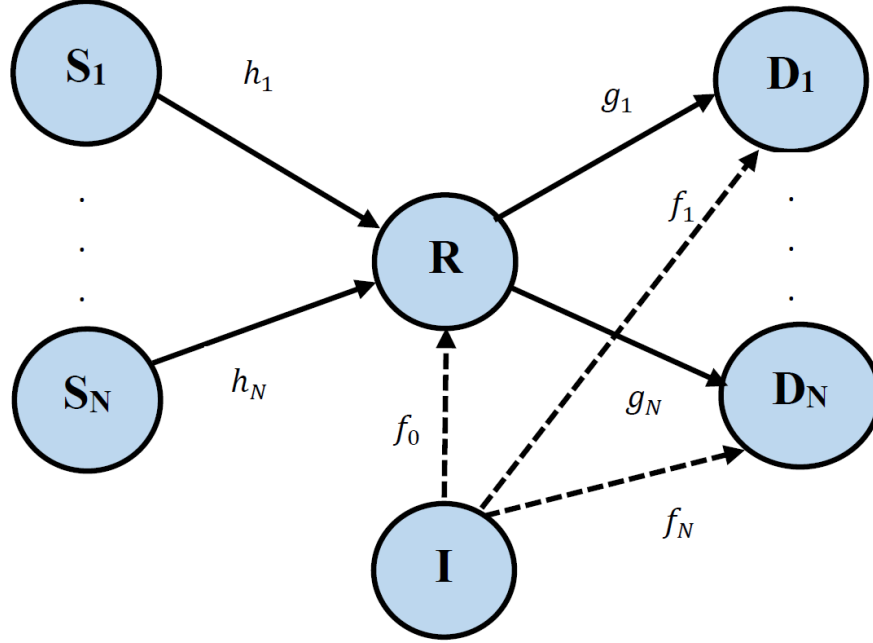
Figure 4.1: System Model

$\frac{T}{2}$ is for the source-relay pair communication and the remaining $\frac{T}{2}$ is for the relay-destination pair communication. Each source communicates with its corresponding destination in a different mini-slot $\frac{T}{N}$, than the other adopting the orthogonality principle; the first $\frac{T}{2N}$ is for $\mathbf{S}_i - \mathbf{R}$ communication while the remaining $\frac{T}{2N}$ is for $\mathbf{R} - \mathbf{D}_i$ communication, as illustrated in Fig. 4.2. All link gains are assumed to be independent and each experiences Rayleigh block fading [37]-[39]. The relay harvests RF energy from the source transmissions based on the PSR protocol since it was found to outperform the TSR protocol [19].

In the PSR protocol, the relay splits the power of the received signal from the i-th transmitter, i.e., $P_{s,i}$, into two streams throughout its dedicated mini-slot $\frac{T}{2N}$. The portion $\rho_i P_{s,i}$ is used for energy harvesting, while the remaining portion $(1 - \rho_i)P_{s,i}$ is used for information decoding, where ρ_i is the PS ratio of the i-th user pair. The power required at the relay for information processing is assumed to be negligible

Figure 4.2: Time Slot Structure

compared to the power required for signal transmission from the relay to the required destination [13].

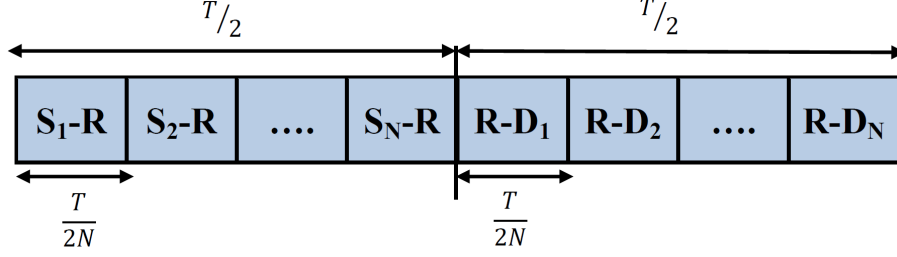The channel gains from the sources to the relay and from the relay to the destinations are denoted by h_i, each with a mean parameter λ_i, and g_i, each with mean parameter ω_i, respectively. The link gain from interferer $\mathbf{I}$ and relay $\mathbf{R}$ is denoted by f_0, with a mean parameter ν_0, while the link gains to the different destinations are denoted by f_i, each with a mean parameter ν_i, where $i = 1, ..., N$. The distance between $\mathbf{I}$ and $\mathbf{R}$ is denoted by d_1, while the distance between $\mathbf{I}$ and the destination $\mathbf{D}_i$ is denoted by $d_{2,i}$. On the other hand the distance between the source $\mathbf{S}_i$ and $\mathbf{R}$ is given by $d_{3,i}$, and the distance between $\mathbf{R}$ and the destination $\mathbf{D}_i$ is given by $d_{4,i}$. We neglect the effect of noise in our model as the interference power is assumed to be much higher than the noise power.

The portion of the received signal from the source node $\mathbf{S}_i$, which is used for information decoding at the relay node is given by

$$y_{r,i} = \sqrt{\frac{(1 - \rho_i) \, P_{s,i}}{d_{3,i}^m}} h_i x_{s,i}, \tag{4.1}$$

where $P_{s,i}$ is the transmission power of the i-th source and $x_{s,i}$ is the signal transmitted by the i-th source where $|x_{s,i}|^2 = 1$. The data rate from the i-th source to

the relay $\mathbf{R}$ can be given as

$$R_{i,r} = \frac{1}{2} \log \left(1 + \frac{(1 - \rho_i) \, P_{s,i} |h_i|^2 d_1^m}{d_{3,i}^m P_\mathcal{I} |f_0|^2} \right), \tag{4.2}$$

where $P_\mathcal{I}$ is the interferer transmit power. Assuming R is the minimum achievable data rate at the relay, then the parameter ρ_i can be adjusted to satisfy $R_{i,r} = R$ as

$$\rho_i^* = 1 - \frac{d_{3,i}^m P_\mathcal{I} |f_0|^2 \left(2^{2R} - 1 \right)}{P_{s,i} |h_i|^2 d_1^m}. \tag{4.3}$$

From (4.3), if the PS ratio ρ_i is chosen such that $\rho_i > \rho_i^*$, there will not be enough power for information decoding leading to unsuccessful decoding at the relay. Therefore to ensure successful decoding at the relay, we need to ensure that $\rho_i \leq \rho_i^*$, given that the statistical CSI is available at the relay. The total energy harvested by the relay should be allocated to different users to achieve a certain overall objective for the relay network. The chosen objective aims at enhancing a desired performance measure, which in turn results in a certain power allocation scheme that has its own effect on the system performance. This will be studied in the following sections. First we consider a non-shared power allocation scheme then we study several shared allocation schemes, followed by a performance comparison for each of the considered schemes.

4.4 Non-Shared Power Allocation Scheme (NSPA)

The simplest way to use the relay's harvested energy is to consider that there is no cooperation between the different source-destination pairs. Then, the energy harvested from the i-th source is used by the DF relay as its transmit power for information transmission to the i-th destination, i.e., the relay transmit power for

the i-th destination is given as

$$P_{r,i} = \frac{\eta \rho_i P_{s,i} |h_i|^2}{d_{3,i}^m}, \tag{4.4}$$

where the transmit powers of all sources are assumed to be the same, i.e. $P_{s,i} = P_s$. This extends the case we studied in Chapter 2 where we had only one source-destination pair, to having N source-destination pairs. For notational simplicity we define $X_i = |H_i|^2$, $Y_i = |G_i|^2$, $Z_i = |F_i|^2$ and $Z_0 = |F_0|^2$ where $|h_i|^2$, $|g_i|^2$, $|f_i|^2$ and $|f_0|^2$ are realizations of the rv's $|H_i|^2$, $|G_i|^2$, $|F_i|^2$ and $|F_0|^2$ respectively. The SIR at the relay and at each of the destinations can be expressed as

$$\Gamma_{R,i} = \frac{P_s (1 - \rho_i) |h_i|^2 d_1^m}{d_{3,i}^m P_\mathcal{I} |f_0|^2} = \frac{\rho_{R_i} X_i}{Z_0}, \tag{4.5}$$

$$\Gamma_{D,i} = \frac{P_{r,i} |g_i|^2 d_{2,i}^m}{d_{4,i}^m P_\mathcal{I} |f_i|^2} = \frac{\rho_{D_i} X_i Y_i}{Z_i}, \tag{4.6}$$

where we assume that $d_{2,i} = d_2$, $d_{3,i} = d_3$ and $d_{4,i} = d_4$ throughout this chapter to simplify our expressions.

The outage probability for the DF relay network is expressed as

$$P_{out} = 1 - Pr \left\{ \Gamma_{R,i} \geq \gamma_{th}, \Gamma_{D,i} \geq \gamma_{th}, \right\}. \tag{4.7}$$

Using the same approach as in Chapter 2, the outage probability and the throughput in the delay-sensitive transmission mode using the PSR protocol can be expressed as

$$P_{out,i} = \frac{c_i}{\lambda_i} e^{\frac{c_i}{\lambda_i}} E_1 \left(\frac{c_i}{\lambda_i} \right) - \frac{c_i}{\lambda_i} e^{a_i c_i} E_1 (a_i c_i) + \frac{1}{a_i \lambda_i}, \tag{4.8}$$

$$\tau_{ds,i} = \frac{T/2N}{T} R_{ds} (1 - P_{out,i}) = \frac{1}{2N} R_{ds} (1 - P_{out,i}), \tag{4.9}$$

where $\rho_{R_i} = \frac{P_s(1-\rho_i)\beta_{1,3}}{P_{\mathcal{I}}}$, $\rho_{D_i} = \frac{\eta\rho_i P_s \beta_{2,4}}{d_3^m P_{\mathcal{I}}}$, $\beta_{1,3} = \frac{d_1^m}{d_3^m}$, $\beta_{2,4} = \frac{d_2^m}{d_4^m}$, $c_i = \frac{\nu_i \gamma_{th}}{\rho_{D_i}\omega_i} = \frac{\gamma_{th}\nu_i d_3^m P_{\mathcal{I}}}{\eta\rho_i P_s \beta_{2,4}\omega_i}$ and $a_i = \frac{\rho_{R_i}}{\gamma_{th}\nu_0} + \frac{1}{\lambda_i} = \frac{P_s(1-\rho_i)\beta_{1,3}}{P_{\mathcal{I}}\gamma_{th}\nu_0} + \frac{1}{\lambda_i}$. Moreover, the optimal PS ratio for the Non-Shared Power Allocation (NSPA) scheme can be found by solving the following problem

$$\max_{\rho_i} \quad R_{tot} = \sum_{i=1}^{N} R_i$$
$$s.t. \quad 0 \le \rho_i \le 1 \tag{4.10}$$

where $R_i = \min\left(\frac{1}{2}\log_2\left(1 + \Gamma_{R,i}\right), \frac{1}{2}\log_2\left(1 + \Gamma_{D,i}\right)\right)$, and is defined as the system rate for the i-th user pair. Therefore the optimal solution is when the $\mathbf{S}_i - \mathbf{R}$ rate is equal to the $\mathbf{R} - \mathbf{D}_i$ rate since all user pairs are independent of each other. The optimal PS ratio for the non cooperative transmission is found as

$$\frac{1}{2}\log_2\left(1 + \Gamma_{R,i}\right) = \frac{1}{2}\log_2\left(1 + \Gamma_{D,i}\right)$$
$$\frac{P_s\left(1 - \rho_{i,NSPA}^*\right)X_i\beta_{1,3}}{P_{\mathcal{I}}Z_0} = \frac{\eta\rho_{i,NSPA}^* P_s X_i Y_i \beta_{2,4}}{d_3^m P_{\mathcal{I}} Z_i}$$
$$\rho_{i,NSPA}^* = \frac{\frac{\beta_{1,3}}{Z_0}}{\frac{\beta_{1,3}}{Z_0} + \frac{\eta\beta_{2,4}Y_i}{d_3^m Z_i}}. \tag{4.11}$$

4.5 Shared Power Allocation

In the shared power allocation schemes the relay harvests energy from the N sources such that the total energy harvested at the relay node and the relay transmit power are given respectively as

$$E_{h_r} = \sum_{i=1}^{N} \frac{\eta\rho_i P_{s,i}|h_i|^2}{d_3^m} \times \frac{T}{2}, \tag{4.12}$$

$$P_r = \frac{E_{h_r}}{T/2} = \sum_{i=1}^{N} \frac{\eta\rho_i P_{s,i}|h_i|^2}{d_3^m}, \tag{4.13}$$

given that $P_{s,i} = P_s$ for all N sources and $\rho_i \leq \rho_i^*$ expressed in (4.3) to ensure successful information decoding at the relay. We wish to study how the total power at the relay should be distributed among the various $\mathbf{R} - \mathbf{D}$ links available. We will consider (1) an equal power allocation scheme, (2) a power allocation scheme which assigns powers to each $\mathbf{R} - \mathbf{D}$ link based on its strength, (3) a power allocation scheme which maximizes the minimum $\mathbf{R} - \mathbf{D}$ rate and (4) a power allocation scheme which maximizes the weighted-sum-rate of all $\mathbf{R} - \mathbf{D}$ links.

4.5.1 Equal Power Allocation (EPA)

In equal power allocation (EPA), the relay distributes the energy harvested from all source transmissions equally among all $\mathbf{R} - \mathbf{D}$ links. The relay transmit power for any of the $\mathbf{R} - \mathbf{D}$ links is expressed as

$$P_r = \frac{E_{h_r}}{T/2} \times \frac{1}{N} = \frac{1}{N} \sum_{i=1}^{N} \frac{\eta \rho P_s |h_i|^2}{d_3^m}, \tag{4.14}$$

where we assume that the different $\mathbf{S} - \mathbf{R}$ channel gains are independent and identically distributed, i.e. $\lambda_i = \lambda$. Compared to the NSPA scheme, this scheme can ensure that the $\mathbf{R} - \mathbf{D}$ links with poor channel conditions can experience reduced chances of outages without having to know the $\mathbf{R} - \mathbf{D}$ channel information. From (4.3), we find the optimal PS ratio ensuring successful decoding at the relay is the same for all $\mathbf{S} - \mathbf{R}$ links. The SIRs at the relay and each of the destinations are

$$
\begin{aligned}
\Gamma_{R,i} &= \frac{P_s \left(1 - \rho\right) |h_i|^2 \beta_{1,3}}{P_{\mathcal{I}} |f_0|^2} = \frac{\rho_R X_i}{Z_0}, &(4.15) \\
\Gamma_{D,i} &= \frac{P_{r,i} |g_i|^2 \beta_{2,4}}{P_{\mathcal{I}} |f_i|^2} = \frac{1}{N} \times \frac{\eta \rho P_s |g_i|^2 \beta_{2,4}}{d_3^m P_{\mathcal{I}} |f_i|^2} \times \sum_{i=1}^{N} |h_i|^2 \\
&= \rho_D \frac{Y_i W}{Z_i}, &(4.16)
\end{aligned}
$$

where $W = \sum_{i=1}^{N} |h_i|^2$, and the sum of N independent exponential rv's has a chi-square distribution. Assuming $\lambda_1 = \lambda_2 = ... = \lambda_i = \lambda$, the PDF and the CDF of W are given respectively as

$$f_W(w) = \frac{w^{N-1}e^{-\frac{w}{\lambda}}}{\Gamma(N)(\lambda)^N}, \tag{4.17}$$

$$F_W(w) = \frac{\Gamma(N, \frac{w}{\lambda})}{\Gamma(N)}, \tag{4.18}$$

where $\Gamma(.)$ denotes the complete gamma function and $\Gamma(.,.)$ denotes the incomplete gamma function [28]. From (4.15) and (4.16), we see that in the EPA scheme $\Gamma_{R,i}$ and $\Gamma_{D,i}$ are independent. Hence the outage joint probability in (4.7) can be expressed as

$$P_{out,i} = 1 - (Pr\{\Gamma_{R,i} \geq \gamma_{th}\} \times Pr\{\Gamma_{D,i} \geq \gamma_{th}\}). \tag{4.19}$$

An expression for the outage probability can be found as

$$\mathcal{I}_{R,i} = Pr\left\{\frac{\rho_R X_i}{Z_0} \geq \gamma_{th}\right\} = \frac{\rho_R \lambda_i}{\gamma_{th}\nu_0 + \rho_R \lambda_i}, \tag{4.20}$$

$$\mathcal{I}_{D,i} = Pr\left\{\rho_D \frac{Y_i W}{Z_i} \geq \gamma_{th}\right\}$$

$$= \frac{1}{\Gamma(N)a^N} \int_0^\infty \frac{W^N}{W+c_i} \times e^{-aW} dW, \tag{4.21}$$

where the probability expression in (4.20) is evaluated similarly as in (3.7), $c_i = \frac{\gamma_{th}\nu_i}{\rho_D \omega_i}$ and $a = \frac{1}{\lambda}$. The integral in (4.21) can be approximated as follows [27]

$$\mathcal{I}_{D,i} = \frac{1}{\Gamma(N)a^N} \times \left[(-1)^{N-1}c_i^N e^{c_i a} Ei(-c_i a) + \sum_{k=1}^{N}(k-1)!(-c_i)^{N-k}a^{-k}\right]. \tag{4.22}$$

The outage probability expression is obtained by substituting (4.20) and (4.22) into (4.19). The achievable throughput for the delay-sensitive transmission mode

(refer to Subsection 2.4.2) can be expressed as

$$\tau_{ds,i} = \frac{T/2N}{T} R_{ds}(1 - P_{out,i}) = \frac{1}{2N} R_{ds}(1 - P_{out,i}). \qquad (4.23)$$

4.5.2 $\mathbf{R} - \mathbf{D}$ Channel Dependent Power Allocation (RDCD)

In the $\mathbf{R} - \mathbf{D}$ channel dependent (RDCD) scheme the relay's harvested power is divided among its links to the different destinations unequally, such that the power allocated for the i-th link depends on the $\mathbf{R} - \mathbf{D}_i$ channel gain as well as the corresponding interference channel gain, i.e., $|g_i|^2$ and $|f_i|^2$ respectively. In this scheme we assume that the statistical CSI is available at the relay. The data rate at the i-th destination is

$$R_{i,d} = \frac{1}{2} \log_2 (1 + \Gamma_{D,i}) = \frac{1}{2} \log_2 \left(1 + \frac{P_{r,i}|g_i|^2 \beta_{2,4}}{P_{\mathcal{I}}|f_i|^2} \right). \qquad (4.24)$$

For a minimum achievable data rate, $R_{i,d} = R$, the minimum required power, $P_{r,i}$, for the $\mathbf{R} - \mathbf{D}_i$ channel is given by

$$P_{r,i} = \left(2^{2R} - 1 \right) \frac{P_{\mathcal{I}}|f_i|^2}{\beta_{2,4}|g_i|^2}. \qquad (4.25)$$

Assuming that the N sources are capable of delivering information to the relay reliably, and that the SIR at $\mathbf{D}_1$ is better than the SIR at $\mathbf{D}_2$ on average, all the way till $\mathbf{D}_N$, then the minimum required relay transmission power for the N destinations can be expressed as

$$\left(2^{2R} - 1 \right) \frac{P_{\mathcal{I}}|f_N|^2}{\beta_{2,4}|g_N|^2} \geq \cdots \geq \left(2^{2R} - 1 \right) \frac{P_{\mathcal{I}}|f_1|^2}{\beta_{2,4}|g_1|^2}. \qquad (4.26)$$

In the RDCD scheme, the relay allocates the minimum required power to the

best $\mathbf{R} - \mathbf{D}$ channel, i.e., the one with strongest channel gain and lowest interference on average, by allocating a power of $\frac{\left(2^{2R}-1\right)P_{\mathcal{I}}|f_1|^2}{\beta_{2,4}|g_1|^2}$ to it, assuming the average channel gains are available at the relay node. This process is repeated for the next best $\mathbf{R} - \mathbf{D}$ channel until either destination $\mathbf{D}_N$ is allocated its minimum required power, or until there is not enough energy left at the relay. In case the relay has some energy after allocating the minimum required powers to each destination, the residual energy at the relay will be equally distributed between all $\mathbf{R} - \mathbf{D}$ channels. Distributing the residual energy increases the SIR among the different $\mathbf{R} - \mathbf{D}$ links, which helps to reduce the outages at the corresponding $\mathbf{R} - \mathbf{D}$ links. To derive an expression for the outage probability, we first express the SIRs at the relay due to the source $\mathbf{S}_i$'s transmission, as well as at the destination $\mathbf{D}_i$ respectively as

$$\Gamma_{R,i} = \frac{P_s\left(1-\rho\right)|h_i|^2 d_1^m}{d_3^m P_{\mathcal{I}}|f_0|^2} = \frac{\rho_R X_i}{Z_0}, \tag{4.27}$$

$$\Gamma_{D,i} = \frac{P_{r,i}|g_i|^2 d_2^m}{d_4^m P_{\mathcal{I}}|f_i|^2} = \frac{P_{r,i}\rho_D Y_i}{Z_i}. \tag{4.28}$$

Since $\Gamma_{R,i}$ in (4.27) and $\Gamma_{D,i}$ in (4.28) are independent, the outage probability and the throughput in the delay-sensitive transmission mode are given respectively by

$$P_{out,i} = 1 - \left(Pr\left\{\Gamma_{R,i} \geq \gamma_{th}\right\} \times Pr\left\{\Gamma_{D,i} \geq \gamma_{th}\right\}\right)$$

$$= 1 - \left(\left\{\frac{\rho_R \lambda_i}{\gamma_{th}\nu_0 + \rho_R \lambda_i}\right\} \times \left\{\frac{P_{r,i}\rho_D \omega_i}{\gamma_{th}\nu_i + P_{r,i}\rho_D \omega_i}\right\}\right), \tag{4.29}$$

$$\tau_{ds,i} = \frac{T/2N}{T} R_{ds}(1 - P_{out,i}) = \frac{1}{2N} R_{ds}(1 - P_{out,i}). \tag{4.30}$$

4.5.3 Max-Min $\mathbf{R} - \mathbf{D}$ Rate Power allocation (MMRD)

In the max-min $\mathbf{R} - \mathbf{D}$ rate (MMRD) scheme, the relay's harvested power is unequally divided among its links to the different destinations, in such a way that the minimum destination SIR is maximized, i.e. the worst $\mathbf{R} - \mathbf{D}$ rate is maximized.

This can be expressed as

$$\max_{\theta_i, i=1,\dots,N} \quad \min_{i=1,\dots,N} \{R_{i,d}\}$$
$$s.t. \qquad \sum_{i=1}^{N} \theta_i = 1 \tag{4.31}$$

where

$$R_{i,d} = \frac{1}{2} \log_2 \left(1 + \Gamma_{D,i}\right), \tag{4.32}$$

and

$$\Gamma_{D,i} = \frac{\theta_i P_r |g_i|^2 d_2^m}{d_4^m P_{\mathcal{I}} |f_i|^2} = \frac{\theta_i \eta \rho P_s W Y_i \beta_{2,4}}{d_3^m P_{\mathcal{I}} Z_i} = \frac{\theta_i \rho_D W Y_i}{Z_i}. \tag{4.33}$$

The parameter θ_i is the fraction of the total relay transmit power P_r allocated to its corresponding $\mathbf{R} - \mathbf{D}_i$ link. It is obtained by solving the optimization problem in (4.31). In order to get a closed-form expression for the optimization variable θ_i, we solve the previous optimization problem as follows [40]

$$\max_{\theta_i, i=1,\dots,N} \quad t$$
$$s.t. \qquad t \leq R_{i,d}$$
$$\sum_{i=1}^{N} \theta_i = 1 \quad , i = 1, \dots, N.$$

Since our aim is to maximize t, then the maximum will occur when the first inequality constraint becomes an equality, i.e. $t = R_{i,d} = \frac{1}{2} \log_2 \left(1 + a_i \theta_i\right)$, where $a_i = \frac{\eta \rho P_s \beta_{2,4} W Y_i}{d_3^m P_{\mathcal{I}} Z_i}$. Therefore

$$\theta_i = \frac{2^{2t} - 1}{a_i}, \tag{4.34}$$

then by substituting the expression for θ_i in the equality constraint, we get an

expression for t and θ_i^* as

$$t = \frac{1}{2} \log_2 \left(1 + \frac{1}{\sum_{i=1}^N \frac{1}{a_i}} \right), \tag{4.35}$$

$$\theta_i^* = \frac{1}{a_i \left(\sum_{i=1}^N \frac{1}{a_i} \right)}. \tag{4.36}$$

Now we want to derive an expression for the outage probability. Note that the SIR at the relay as a result of the source $\mathbf{S}_i$'s transmission is the same as that defined in (4.27), while the SIR at the destination $\mathbf{D}_i$ is given by (4.33). Since $W = \sum_{i=1}^N X_i$ is the sum of N exponential rv's, its pdf is given by (4.17). Therefore $\Gamma_{R,i}$ and $\Gamma_{D,i}$ are independent and the outage probability can be obtained as

$$\mathcal{I}_{R,i} = Pr\left\{ \frac{\rho_R X_i}{Z_0} \geq \gamma_{th} \right\} = \frac{\rho_R \lambda_i}{\gamma_{th} \nu_0 + \rho_R \lambda_i}, \tag{4.37}$$

$$\mathcal{I}_{D,i} = Pr\left\{ \theta_i \rho_D \frac{Y_i W}{Z_i} \geq \gamma_{th} \right\} = \frac{1}{\Gamma(N) a^N} \int_0^\infty \frac{W^N}{W + c_i} \times e^{-aW} dW$$

$$= \frac{1}{\Gamma(N) a^N} \times \left[(-1)^{N-1} c_i^N e^{c_i a} Ei(-c_i a) + \sum_{k=1}^N (k-1)!(-c_i)^{N-k} a^{-k} \right], \tag{4.38}$$

$$P_{out,i} = \frac{\rho_R \lambda_i}{\Gamma(N) a^N \left(\gamma_{th} \nu_0 + \rho_R \lambda_i \right)} \times \left[(-1)^{N-1} c_i^N e^{c_i a} Ei(-c_i a) + \sum_{k=1}^N (k-1)!(-c_i)^{N-k} a^{-k} \right], \tag{4.39}$$

where $c_i = \frac{\gamma_{th} \nu_i}{\theta_i \rho_D \omega_i}$ and $a = \frac{1}{\lambda}$. The throughput is obtained by substituting the expression of $P_{out,i}$ in (4.39) in (4.30). Note that the MMRD power allocation scheme achieves the highest fairness of all schemes at the cost of improving the performance of the worst user only, which may lead to the degradation of the total network throughput.

4.5.4 Weighted-Sum-Rate Maximization of all $\mathbf{R} - \mathbf{D}$ links Power Allocation

In the weighted-sum-rate maximization (WSRM) scheme, the relay's total harvested power is unequally divided among its links to the different destinations, in such a way that the weighted-sum-rate of all the $\mathbf{R} - \mathbf{D}$ links is maximized. The WSRM can achieve certain fairness for different $\mathbf{R} - \mathbf{D}$ links by allocating large weights to links with bad channel conditions, while maintaining good network performance, and it can be formulated as follows

$$\max_{\theta_i, i=1,\dots,N} \quad \sum_{i=1}^{N} \mu_i R_{i,d}$$
$$s.t. \quad \sum_{i=1}^{N} \theta_i = 1 \tag{4.40}$$

where μ_i denotes the weight allocated to the link $\mathbf{R} - \mathbf{D}_i$. The optimization variable θ_i is the fraction of the total harvested power by the relay allocated to the link $\mathbf{R} - \mathbf{D}_i$, and $R_{i,d}$ is the achieved rate at the link $\mathbf{R} - \mathbf{D}_i$, which is expressed in Subsection 4.5.3 in (4.32) and (4.33). Now we rewrite the above optimization problem in terms of the variable θ_i as

$$\max_{\theta_i, i=1,\dots,N} \quad \sum_{i=1}^{N} \frac{\mu_i}{2} \log_2 \left(1 + a_i \theta_i\right)$$
$$s.t. \quad \sum_{i=1}^{N} \theta_i = 1 \tag{4.41}$$

where $a_i = \frac{\eta \rho P_s \beta_{2,4} W Y_i}{d_3^m P_{\mathcal{I}} Z_i}$.

The objective function in (4.41) is concave and the constraint is affine in terms of the optimization variable θ_i thus it is a convex problem. The Lagrangian function

[40] is thus given by

$$\mathcal{L}\left(\theta_i, \lambda\right) = \frac{1}{2} \sum_{i=1}^{N} \mu_i \log\left(1 + a_i \theta_i\right) - \lambda \left(\sum_{i=1}^{N} \theta_i - 1\right). \tag{4.42}$$

Since the problem is convex, we can find its optimal solution by using Karush-Kuhn-Tucker (KKT) conditions which are

$$\frac{d\mathcal{L}\left(\theta_i, \lambda\right)}{d\theta_i} = \left(\frac{\mu_i}{2} \times \frac{a_i}{1+a_i\theta_i}\right) - \lambda = 0, \tag{4.43}$$

$$\sum_{i=1}^{N} \theta_i = 1. \tag{4.44}$$

After some mathematical manipulations we get an expression of θ_i^* as

$$\theta_i^* = \frac{\mu_i \left(1 + \sum_i \frac{1}{a_i}\right)}{\sum_{i=1}^{N} \mu_i} - \frac{1}{a_i}. \tag{4.45}$$

Since $\theta_i^* > 0$, then by looking at (4.45) the weights should be chosen such that

$$\frac{\mu_i}{\sum_{i=1}^{N} \mu_i} > \frac{1}{a_i \left(1 + \sum_i \frac{1}{a_i}\right)}. \tag{4.46}$$

The choice of μ_i's can be fixed and chosen such that channels with unfavorable conditions have larger μ_i's than those with better conditions as discussed earlier. We also examine the dynamic assignment of μ_i's to the different $\mathbf{R} - \mathbf{D}$ links according to some criteria. The criteria we use for choosing the weights is dividing the sum of rates achieved at all $\mathbf{R} - \mathbf{D}$ links by the rate achieved at the intended $\mathbf{R} - \mathbf{D}_i$ link, given that the condition in (4.46) is satisfied. The dynamic weights are assigned as follows

$$\mu_i = \frac{\sum_{i=1}^{N} R_{i,d}}{R_{i,d}}, \tag{4.47}$$

which shows that $\mathbf{R} - \mathbf{D}$ links achieving lower rates are assigned larger weights than

$\mathbf{R} - \mathbf{D}$ links achieving higher rates.

The outage probability and the throughput using the WSRM scheme are evaluated similarly as in the MMRD scheme. The outage probability is given in (4.39). We then substitute $P_{out,i}$ in (4.30) to evaluate the throughput, i.e., $\tau_{ds,i} = \frac{1}{2N} R_{ds}(1 - P_{out,i})$. The similarity between the MMRD and the WSRM schemes can be observed since $\Gamma_{R,i}$ and $\Gamma_{D,i}$ are the same for both schemes, and are given by (4.27) and (4.33) respectively. The only difference is in evaluating the variable θ_i, i.e., the power allocated for each $\mathbf{R} - \mathbf{D}_i$ link, which is different for each scheme since the WSRM objective is different than the MMRD objective in (4.31). It would also be interesting to look at performance measures other than the outage probability/throughput such as the fairness which can be measured in terms of the fairness index given by [41]

$$F_I = \frac{\left(\sum_{i=1}^{N} R_{i,d}\right)^2}{N \times \sum_{i=1}^{N} R_{i,d}^2}. \tag{4.48}$$

4.6 Numerical Results

In this section, we compare the performances of the five different power allocation schemes discussed in Sections 4.4 and 4.5, in terms of their outage probabilities, throughputs, and the fairness. To simplify our expressions, we assumed that the distances between all source nodes and the relay node are equal, the distances between the relay node and all destination nodes are equal, and the distances between the interferer node and all destination nodes are equal. The number, N, of source-destination pairs is set to 5, and we assume that the $\mathbf{R} - \mathbf{D}_i$ channel quality is non-increasing with $i \in \{1, 2, ..., 5\}$, i.e., the $\mathbf{R} - \mathbf{D}_5$ channel has the worst quality. The channel gains from the sources to the relay are assumed to be independent and identically distributed, i.e, $\lambda_1 = \lambda_2 = ... = \lambda_5 = \lambda$. The energy harvesting efficiency

$\eta = 1$ and the SIR threshold value $\gamma_{th} = 0$ dB. We ensure that the power-split ratio $\rho_i \leq \rho_i^*$ throughout this section for the different studied allocation schemes to ensure successful information decoding at the relay node (as required in (4.3)). The parameter values used in our simulation results are summarized in Table 4.1.

Parameter	Value
η	1
m	4
γ_{th}	0 dB
P_s	2 dBm
d_1	3 m
d_2	2 m
d_3	1.5 m
d_4	1 m

Table 4.1: Simulation parameter values

A plot of the outage probability versus ρ for the NSPA and the EPA schemes is shown in Fig. 4.3 for all 5 $\mathbf{S} - \mathbf{R} - \mathbf{D}$ links. It can be seen that there is a match between the simulation results and the analytical results. The results show that the EPA scheme has a lower outage probability than the NSPA scheme for all 5 $\mathbf{S} - \mathbf{R} - \mathbf{D}$ channels. This shows that $\mathbf{R} - \mathbf{D}$ links with poor channels will experience reduced outage probabilities when considering the EPA scheme versus the NSPA scheme. The observed performance improvement can be achieved without the need to know the $\mathbf{R} - \mathbf{D}$ statistical channel CSI for the EPA scheme, making it an attractive power allocation scheme.
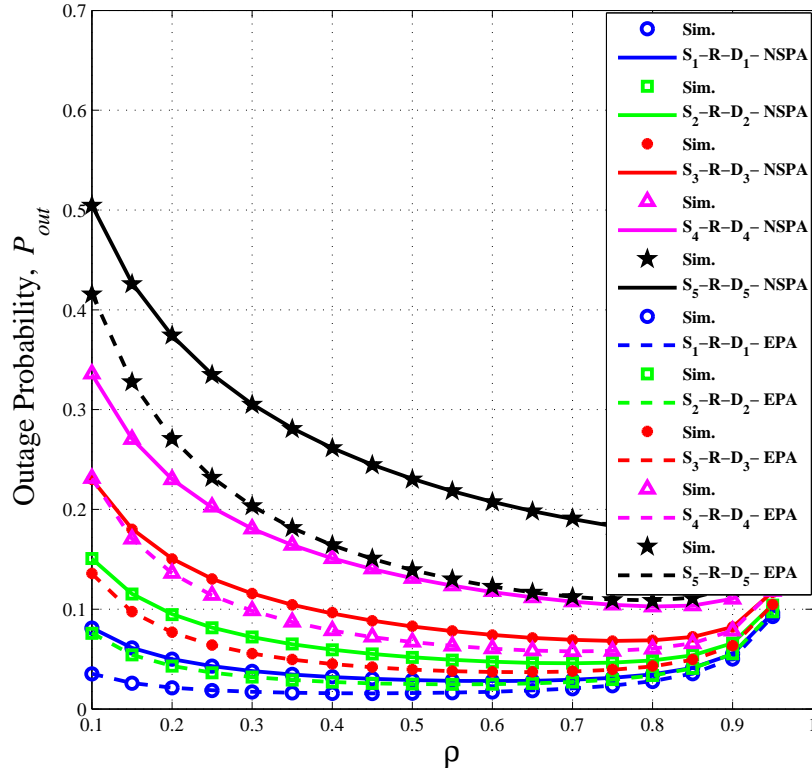
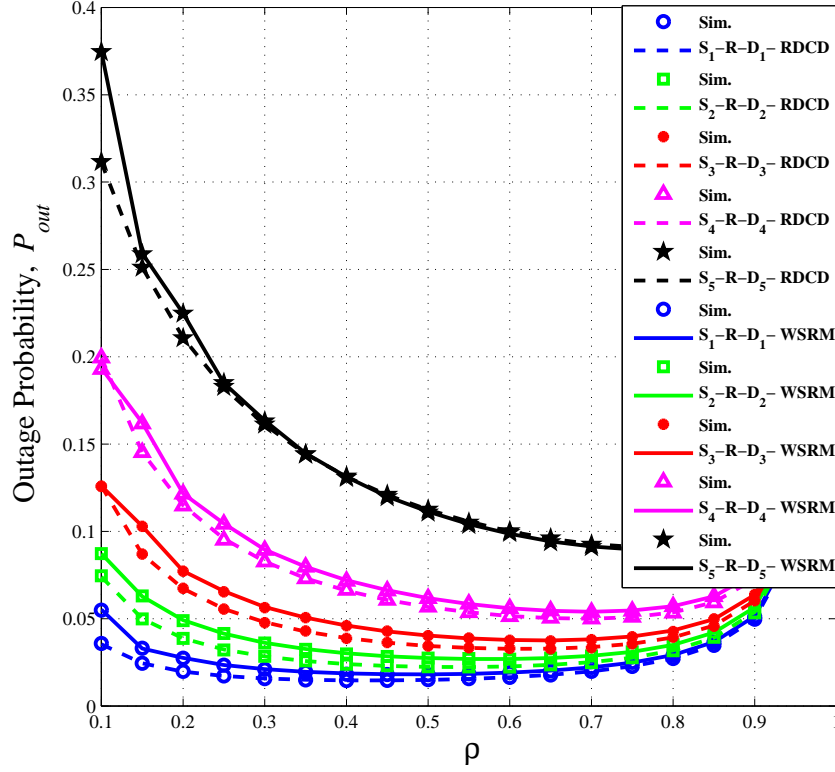Figure 4.3: Outage Probability versus ρ for the NSPA and the EPA schemes

In Fig. 4.4, we compare the outage probability of the EPA and the RDCD schemes as discussed in Subsections 4.5.1 and 4.5.2 respectively. It can be seen that the channels with high SIRs experience nearly the same outage probability with the two schemes. On the other hand, the RDCD scheme outperforms the EPA scheme in terms of outage probability for channels with low SIRs. This comes at the cost of higher complexity since the RDCD scheme requires the relay or another central controller node to know the statistical CSI of all wireless links.
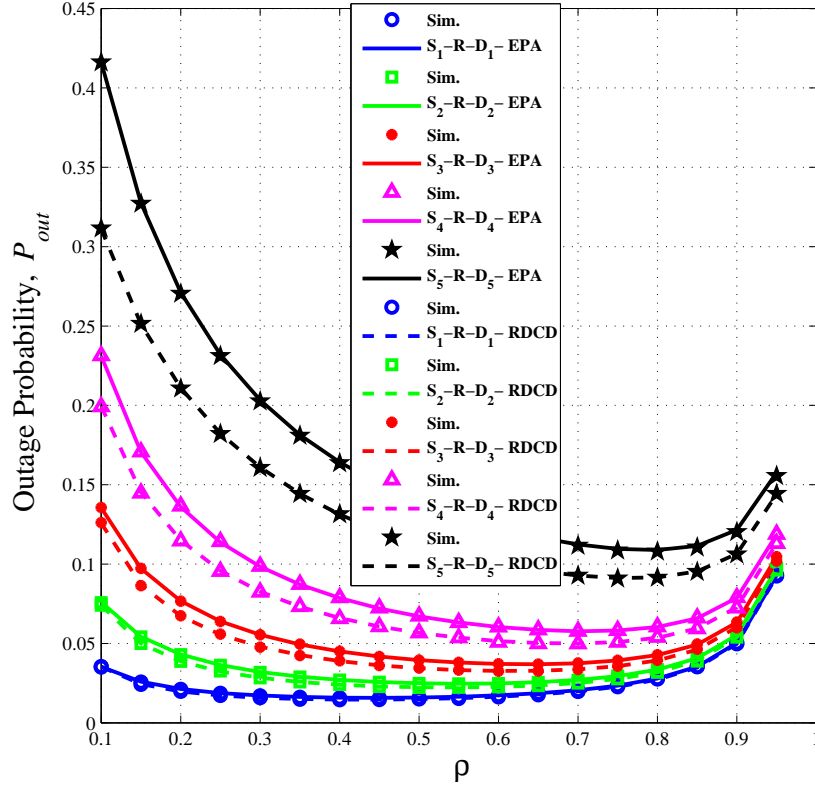
Figure 4.4: Outage Probability versus ρ for the EPA and the RDCD schemes

In Fig. 4.5, we show the outage probabilities of the MMRD and the RDCD schemes. Recall that the MMRD is a max-min rate scheme. As expected, the MMRD scheme results in the same outage probability for all 5 $\mathbf{S} - \mathbf{R} - \mathbf{D}$ links. Note that using the MMRD scheme results in a lower outage probability for the $\mathbf{S}_5 - \mathbf{R} - \mathbf{D}_5$ link only, i.e., worst channel, while the remaining $\mathbf{S}_i - \mathbf{R} - \mathbf{D}_i$ links experience increased outage probabilities. Therefore the MMRD rate scheme is shown to be the fairest scheme so far but this may come at the cost of increased outage probability.
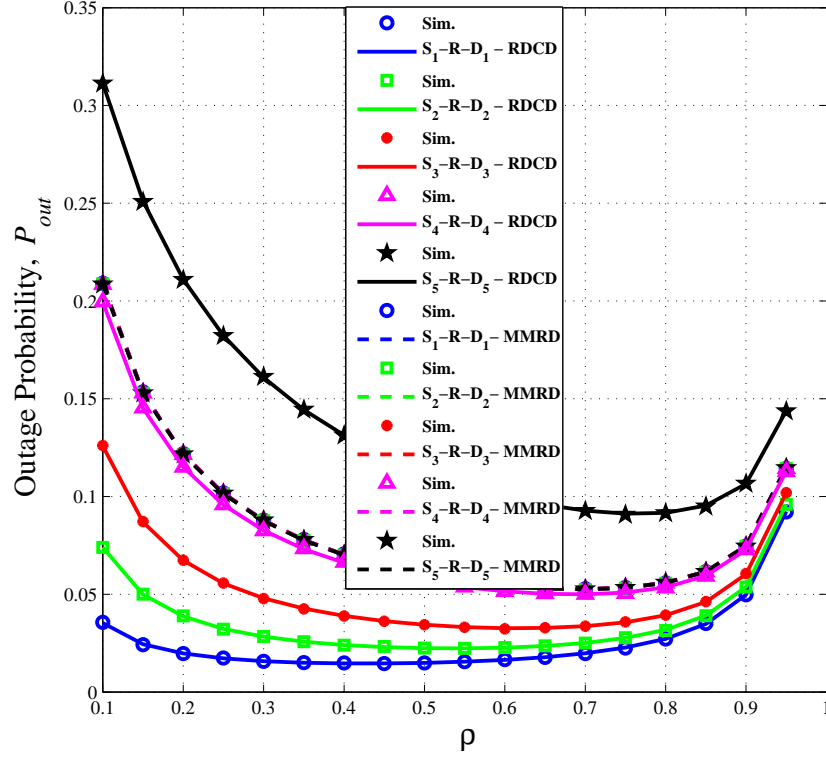
Figure 4.5: Outage Probability versus ρ for the MMRD and the RDCD schemes

Since the RDCD scheme outperforms all other schemes considered so far, in terms of reduced outage probability, we compare it against the WSRM scheme in Fig. 4.6. Recall that in WSRM the weights change dynamically as proposed in (4.47). Fig. 4.6 shows that the RDCD scheme is still superior in terms of outage probability. However, the WSRM scheme achieves a better performance than the NSPA, EPA and MMRD schemes. Comparing Figs. 4.6 and 4.4 it can be seen that the EPA scheme yields better outage probability than the WSRM scheme for the high SIR links, namely $\mathbf{S}_1-\mathbf{R}-\mathbf{D}_1$ and $\mathbf{S}_2-\mathbf{R}-\mathbf{D}_2$.

Figure 4.6: Outage Probability versus ρ for the RDCD and the WSRM schemes

In order to illustrate the effect of using constant weights versus dynamic weights in the WSRM scheme, we compare their outage probabilities in Fig. 4.7. The choice of the constant weights values is done such that larger weights are assigned to links with worse channel conditions to reduce their outage probability. This comes at the cost of increased outage probabilities for links with lower weights. From extensive simulation results, we found the constant weights which achieve an average outage probability ± 0.01 to ± 0.04 compared to other schemes are, $\mu_1 = 1$, $\mu_2 = 1.5$, $\mu_3 = 2$, $\mu_4 = 2.5$ and $\mu_5 = 3$. We also use those values as the initial values for the dynamic weights which are then updated using (4.47). Fig. 4.7 shows that using constant μ_i's yields a slightly lower outage probability than using dynamic μ_i's for links with

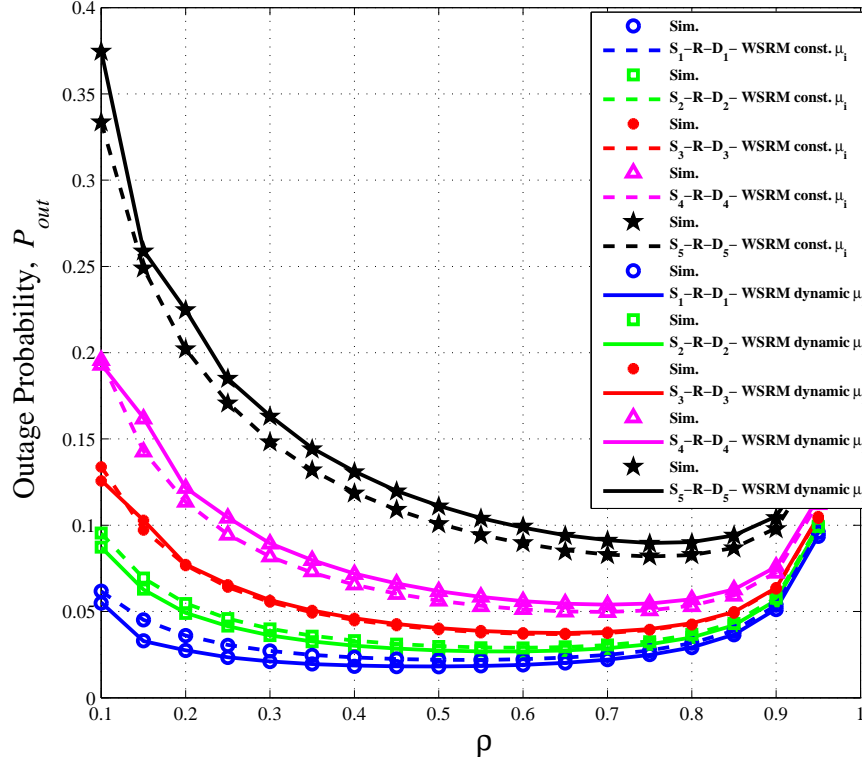bad channel conditions, and slightly higher outage probability for links with better channel conditions.

Figure 4.7: Outage Probability versus ρ for the WSRM with dynamic and constant μ_i's

From Figs. 4.4 - 4.7, we observe that the RDCD scheme yields the best outage probability performance, followed by the WSRM scheme with dynamic weights with a slightly increased performance than the WSRM using constant weights for the links with high SIR, while for the links with low SIR the WSRM with constant weights outperforms the one with dynamic weights. Finally the EPA scheme comes at the end with the highest outage probability for low SIR links, however, it has a similar performance as the RDCD scheme for links with high SIRs.
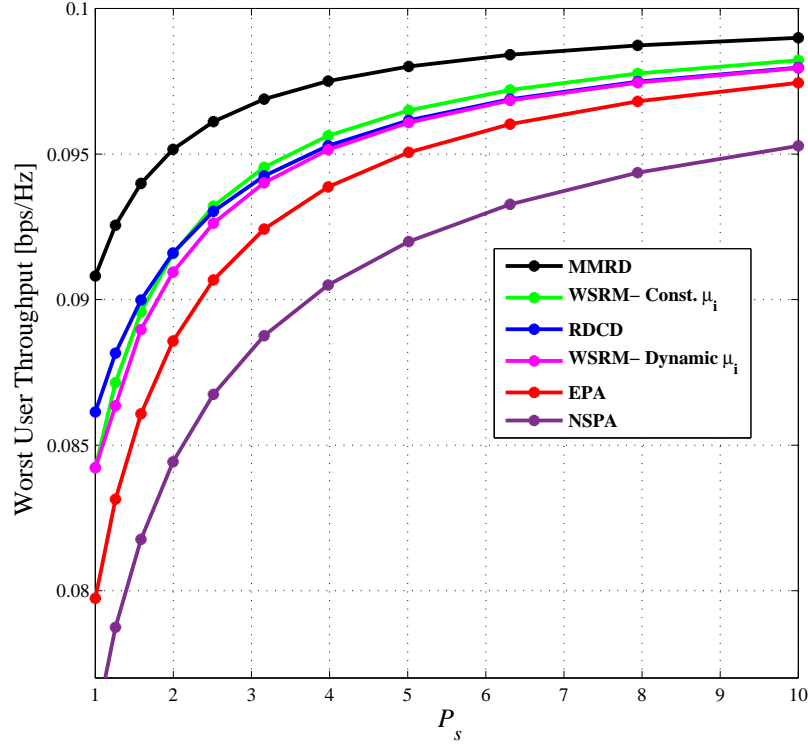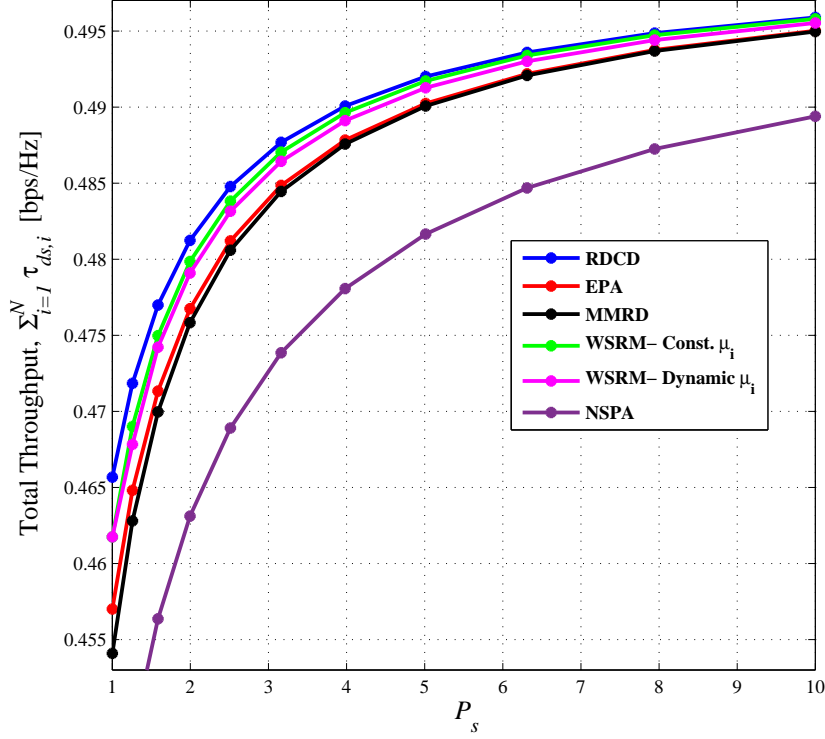
Figure 4.8: Worst user throughput versus P_s

Fig. 4.8 shows the throughput of the worst user as a function of the source power, P_s, for the five power allocation schemes. It is observed that the MMRD scheme results in the highest worst user throughput. This is expected since it tries to maximize the worst $\mathbf{R} - \mathbf{D}$ rate. The NSPA scheme has the lowest worst user throughput. The next lowest worst user throughput is achieved by the EPA scheme, due to the fact that it allocates an equal amount of power to each link regardless of the channel condition. The RDCD scheme and the WSRM scheme with dynamic and constant weights have similar performance in terms of the worst user throughput.

Figure 4.9: Total network throughput versus P_s

In Fig. 4.9, we show the total network throughput, i.e., $\sum_{i=1}^{N} \tau_{ds,i}$, as a function of the source power, P_s, for the five power allocation schemes. It can be seen that the NSPA scheme yields the worst network throughput. The next worst network throughput is achieved by the MMRD scheme, as its objective is to enhance the worst user performance. The best network throughput is achieved by the RDCD scheme. The next best performance is achieved by the WSRM scheme with a slightly lower network throughput than the RDCD scheme.

In practice, it is important to look at other performance measures for the presented power allocation schemes, such as the fairness index as defined in (4.48) and plotted in Fig. 4.10 versus ρ. As expected, the MMRD scheme is the fairest among

all schemes at the cost of a lower throughput. The next best allocation scheme achieving fairness is the WSRM with constant μ_i's first, followed by the WSRM with dynamic μ_i's. On the other hand the least fair scheme is the EPA. Table 4.2 shows the rankings of the different shared allocation schemes in terms of throughput, fairness and outage probability. Note that the performance of the WSRM scheme depends on the choice of the weights, which we have chosen to achieve a reasonable average outage probability compared to other schemes.
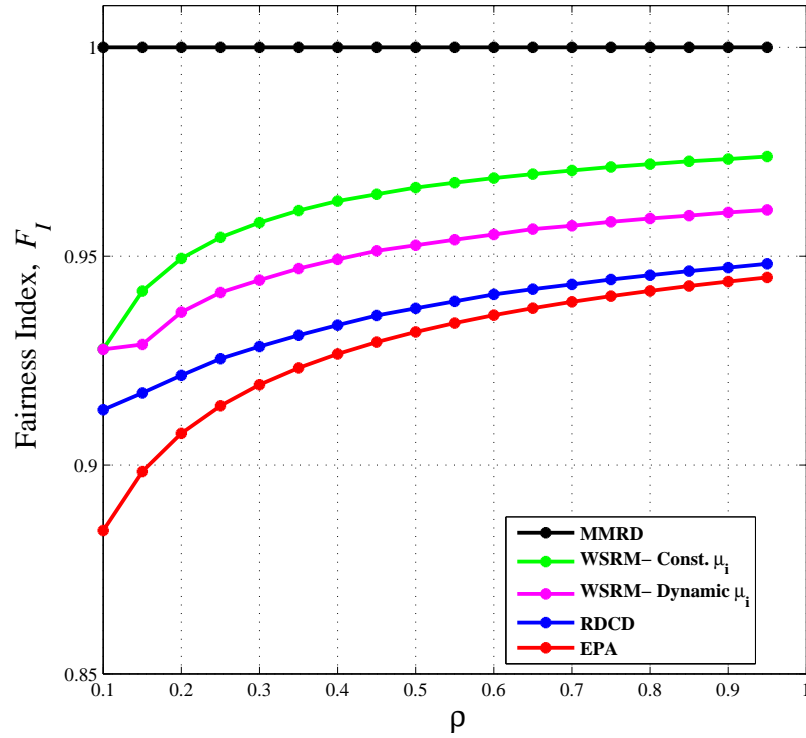

Figure 4.10: Fairness Index versus ρ

Scheme	Total Through-put	Fairness	Outage for high SIR links	Outage for low SIR links	Average Outage
EPA	Poor	Worst	Good	Worst	Poor
RDCD	Best	Poor	Best	Best	Best
MMRD	Worst	Best	Worst	Best (for lowest SIR only)	Worst
WSRM dy-namic μ_i	Average	Average	Average	Average	Average
WSRM constant μ_i	Good	Good	Poor	Good	Good

Table 4.2: Comparison between different shared allocation schemes - NSPA worst of all

4.7 Summary

Different power allocation schemes for a DF WRN have been studied, where multiple source-destination pairs communicate via an energy-constrained relay which harvests RF energy from the source transmissions. Expressions for the outage probability and the throughput in the delay-sensitive transmission mode have been derived for each power allocation scheme. Shared power allocation schemes have been found to outperform the non-shared allocation scenario. Moreover fairness has been considered as a performance measure to compare between different shared allocation schemes. Numerical results show an interesting tradeoff between the throughput and the fairness of the different shared allocation schemes. The RDCD scheme achieved the highest throughput at the cost of decreased fairness, while the MMRD scheme achieved the best fairness at the cost of overall throughput degradation. In conclusion it is important to decide which performance measure is of higher priority when designing resource allocation schemes, otherwise one can choose an allocation scheme which achieves the best balance between the different considered performance measures.

Chapter 5

Conclusions and Future Work

In this chapter we summarize our contributions and main findings in Section 5.1. In Section 5.2, we outline some possible directions for future work.

5.1 Conclusions

In this thesis we studied RF energy harvesting in wireless cooperative networks in the presence of interference. Our main figures of merit are the outage probability and the throughput for delay-sensitive transmission.

- In Chapter 2, we studied the performance of different energy harvesting relaying protocols in a DF WRN in the presence of an interfering signal. The DF relay is energy-constrained, and harvests RF energy from the source signal using the TSR and the PSR protocols. Based on the TSR and the PSR protocols, we proposed a new hybrid TSR-PSR protocol. We derived closed form expressions for the outage probability, upper and lower bounds, as well as the throughput in the delay-sensitive transmission mode for all three relaying protocols. The results show that the PSR protocol has a better throughput than the TSR for high SIRs. Our proposed hybrid protocol generally yields a better throughput performance than the TSR or PSR protocols when the TS and PS ratios are chosen properly.

- In Chapter 3, we generalized the study in Chapter 2, by considering the effect

of harvesting RF energy by the relay node from both the information signal and the interference signal. We derived the outage probability and the throughput of the three relaying protocols studied. The performance degradation due to neglecting harvesting energy from the interference was examined. The numerical results show that there is a slight performance improvement in terms of throughput and outage probability for the assumed system configuration, in which the RF energy harvested from the source signal is larger than that harvested from the interference signal.

- In Chapter 4, we considered a cooperative WRN where multiple source-destination pairs communicate via a DF relay which harvests energy from the source transmissions in the presence of an interfering signal. The goal is to efficiently distribute the relay's power among different $\mathbf{R} - \mathbf{D}$ links. The outage probability and the throughput in the delay-sensitive transmission mode were derived for several power allocation schemes. Numerical results show that the studied shared allocation schemes outperform the non-shared allocation scheme in terms of outage probability and throughput. Different shared allocation schemes were compared against each other in terms of outage probability, throughput and fairness. The RDCD and the WSRM schemes achieve the best outage and throughput performances but require the knowledge of statistical CSI at the relay node. The results illustrate the tradeoff between the throughput and the fairness of the different shared allocation schemes.

5.2   Future Work

We now outline some possible directions for future research:

- In Chapter 2, we presented a sensitivity analysis to illustrate how the perfor-

mance of the proposed hybrid TSR-PSR protocol changes depending on the choice of the TS and PS ratios. Our results demonstrate that when the TS and the PS parameters are well chosen, the hybrid protocol outperforms both TSR and PSR protocols. Further research on the optimization of these parameters would be useful. For example, analytical expressions for the optimal TS and PS ratios of the hybrid protocol, will provide more insight into its performance advantage over the TSR and PSR protocols.

- The system model in Chapter 2, can be extended to include multiple energy harvesting relay nodes and multiple interferer nodes. The effect of different relay selection schemes on the system performance can then be investigated.

- In Chapter 4, we studied shared allocation schemes which require the relay node to have knowledge of the statistical CSI. This may incur some overhead specially when the system has a large number of users. It would be interesting to study distributed power allocation schemes for cases of imperfect CSI availability, and the tradeoff between the system performance and complexity. The case when instantaneous CSI is available can also be studied, in order to assess the potential performance gain.

- Another interesting future research direction is to consider buffer-aided relaying in the design of energy harvesting cooperative networks [42]. In buffer-aided relaying, the relays adaptively transmit or receive packets in a given time slot based on the instantaneous CSI of the $\mathbf{S} - \mathbf{R}$ and $\mathbf{R} - \mathbf{D}$ channels. In conventional relaying, the relay receives in one time slot and forwards the received information to the destination in the following time slot, regardless of the instantaneous CSI of the $\mathbf{S} - \mathbf{R}$ and $\mathbf{R} - \mathbf{D}$ channels. This rigid scheduling may lead to performance degradation due to the inability of the relay to

exploit link diversity, specially when link qualities vary significantly over time.

Bibliography

[1] Q. C. Li, R. Q. Hu, Y. Qian and G. Wu, "Cooperative Communications for Wireless Networks: Techniques and Applications in LTE-Advanced Systems", *IEEE Wireless Commun. Mag.,* vol.19, no. 2, pp. 22-29, Apr. 2012.

[2] Y.W. Hong,W. J. Huang, F. H. Chiu, and C. C. J. Kuo, "Cooperative communications in resource-constrained wireless networks", *IEEE Signal Process. Mag.,* vol. 24, no. 3, pp. 47-57. May 2007.

[3] A. Nosratinia, T. E. Hunter, and A. Hedayat, "Cooperative communication in wireless networks", *IEEE Commun. Mag.,* vol. 42, no. 10, pp. 74-80, Oct. 2004.

[4] H. J. Visser and R. J. M. Vullers, "RF energy harvesting and transport for wireless sensor network applications: principles and requirements", *in Proc. of the IEEE,* vol. 101, no. 6, pp. 1410-1423, Jun. 2013.

[5] K. Ishibashi and H. Ochiai, "Analysis of instantaneous power distributions for non-regenerative and regenerative relaying signals", *IEEE Trans. Wireless Commun.,* vol. 11, no. 1, pp. 258-265, Jan. 2012.

[6] S. Sudevalayam and P. Kulkarni, "Energy harvesting sensor nodes: Survey and implications", in *Proc. IEEE Commun. Surveys & Tutorials,* vol. 13, no. 3, pp. 443-461, Oct. 2011.

[7] M.A. Marsan, G. Bucalo, A. D. Caro, M. Meo and Y. Zhang, "Towards zero grid

electricity networking: Powering BSs with renewable energy sources", in *Proc. IEEE International Conf. on Communications Workshops (ICC),* 2013, pp. 596-601.

[8] S. Chalasani and J. Conrad, "A survey of energy harvesting sources for embedded systems", in *Proc. IEEE SoutheastCon,* 2008, pp. 442-447.

[9] D. Mishra, S. De, S. Jana, S. Basagni, K. Chowdhury, and W. Heinzelman, "Smart RF energy harvesting communications: challenges and opportunities", *IEEE Commun. Mag.,* vol. 53, no. 4, pp. 70-78, Apr. 2015.

[10] S. Bi, C. K. Ho, and R. Zhang, "Wireless powered communication: opportunities and challenges", *IEEE Wireless Commun. Mag.,* vol.53, no. 4, pp. 117-125, Apr. 2015.

[11] L. Varshney, "Transporting information and energy simultaneously", in *Proc. IEEE International Symposium on Information Theory (ISIT)*, 2008, pp. 1612-1616.

[12] P. Grover and A. Sahai, "Shannon meets Tesla: Wireless information and power transfer", in *Proc. IEEE ISIT,* 2010, pp. 2363-2367.

[13] X. Zhou, R. Zhang, and C. K. Ho, "Wireless information and power transfer: Architecture design and rate-energy tradeoff", *IEEE Trans. on Commun.,* vol. 61, no. 11, pp. 4754-4767, Nov. 2013.

[14] L. Liu, R. Zhang, and K.-C. Chua, "Wireless information transfer with opportunistic energy harvesting", *IEEE Trans. Wireless Commun.,* vol. 12, no. 1, pp. 288-300, Jan. 2013.

[15] R. Zhang and C. K. Ho, "MIMO broadcasting for simultaneous wireless infor-

mation and power transfer", *IEEE Trans. Wireless Commun.,* vol. 12, no. 5, pp. 1989-2001, May 2013.

[16] K. Huang, and X. Zhou, "Cutting the last wires for mobile communications by microwave power transfer", *IEEE Commun. Mag.,* vol. 53, no. 6, pp. 86-93, Jun. 2015.

[17] K. Huang, and V. K. N. Lau, "Enabling wireless power transfer in cellular networks: Architecture, modelling and deployment", *IEEE Trans. Wireless Commun.,* vol. 13, no. 2, pp. 902-912, Feb. 2014.

[18] K. R. Foster, "A world awash with wireless devices: Radio-frequency exposure issues", *IEEE Microwave Mag.,* vol. 14, no. 2, pp. 73-84, Apr. 2013.

[19] A. A. Nasir, X. Zhou, S. Durrani, and R. A. Kennedy, "Relaying protocols for wireless energy harvesting and information processing", *IEEE Trans. Wireless Commun.,* vol. 12, no. 7, pp. 3622-3636, Jul. 2013.

[20] Y. Liu, L. Wang, M. Elkashlan, T. Q. Duong, and A. Nallanathan, "Two-way relaying networks with wireless power transfer: Policies design and throughput analysis", in *Proc. IEEE Global Commun. Conf. (GLOBECOM)*, 2014, pp. 4030-4035.

[21] Y. Gu and S. Aissa, "Interference aided energy harvesting in decode-and-forward relaying systems", in *Proc. IEEE International Conf. on Communications (ICC),* 2014, pp. 5378-5382.

[22] H. Chen, Y. Li, Y. Jiang, Y. Ma, and B. Vucetic, "Distributed power splitting for SWIPT in relay interference channels using game theory", *IEEE Trans. Wireless Commun.,* vol. 14, no. 1, pp. 410-420, Jan. 2015.

[23] L. Hu, C. Zhang, and Z. Ding, "Dynamic power splitting policies for AF relay networks with wireless energy harvesting", in *Proc. IEEE ICC,* 2015, pp. 1-5.

[24] M. M. Butt, A. Nasir, A. Mohamed and M. Guizani, "Trading Wireless Information and Power Transfer: Relay Selection to Minimize the Outage Probability", in *Proc. IEEE Global Conf. on Signal and Info. Processing (GlobalSIP),* 2014, pp. 253-257.

[25] S. Mousavifar, Y. Liu, C. Leung, M. Elkashlan, and T. Duong, "Wireless energy harvesting and spectrum sharing in cognitive radio", in *Proc. IEEE Vehicular Technology Conference (VTC Fall),* 2014, pp. 1-5.

[26] X. Lu, P. Wang, D. Niyato, D. I. Kim, and Z. Han, "Wireless networks with RF energy harvesting: A contemporary survey", *IEEE Commun. Surveys & Tutorials,* vol. 17, no. 2, pp. 757-789, May 2015.

[27] I. S. Gradshteyn and I. M. Ryzhik, *Table of integrals, series, and products,* 4th Edition, Academic Press, Inc., 1980.

[28] M. Abramowitz and I. A. Stegun, *Handbook of Mathematical Functions,* New York, Dover Publications, 1972.

[29] J. G. Proakis, *Digital Communications,* New York, McGraw-Hill, 2000.

[30] S. Guo, Y. Yang and Y. Yang, "Wireless Energy Harvesting and Information Processing in Cooperative Wireless Sensor Networks", in *Proc. IEEE ICC,* 2015, pp. 5392-5397.

[31] Z. Ding, S. M. Perlaza, I. Esnaola and H. V. Poor, "Power Allocation Strategies in Energy Harvesting Wireless Cooperative Networks", *IEEE Trans. Wireless Commun.,* vol. 13, no. 2, pp. 846-860, Jan. 2014.

[32] D. Yang, X. Zhou, L. Xiao and F. Wu, "Energy cooperation in multi-user wireless-powered relay networks", *IET Commun.,* vol. 9, no. 11, pp. 1412-1420, Jul. 2015.

[33] Z. Ding and H. V. Poor, "Cooperative Energy Harvesting Networks With Spatially Random Users", *IEEE Signal Process. Lett.,* vol. 20, no. 12, pp. 1211-1214, Oct. 2013.

[34] K. T. Phan, T. Le-Ngoc, S. A. Vorobyov and C. Tellambura, "Power Allocation in Wireless Multi-User Relay Networks", *IEEE Trans. Wireless Commun.,* vol. 8, no. 5, pp. 2535-2545, May 2009.

[35] K. T. Phan, L. B. Le, S. A.Vorobyov and T. Le-Ngoc, "Centralized and Distributed Power Allocation in Multi-User Wireless Relay Networks", in *Proc. IEEE ICC,* 2009, pp. 1-5.

[36] Q. Cao, Y. Jing and H. V. Zhao, "Power Allocation in Multi-User Wireless Relay Networks through Bargaining", *IEEE Trans. Wireless Commun.,* vol. 12, no. 6, pp. 2870-2882, May 2013.

[37] A. Lazaro, D. Girbau and D. Salinas, "Radio Link Budgets for UHF RFID on Multipath Environments", *IEEE Trans. on Antennas and Propagation,* vol. 57, no. 4, pp. 1241-1251, Apr. 2009.

[38] T. S. Rappaport and C. D. McGillem, "UHF fading in factories", *IEEE J. Select. Areas Commun.,* vol. 7, no. 1, pp. 40-48, Jan. 1989.

[39] T. Q. Wu and H. C. Yang, "On the performance of overlaid wireless sensor transmission with RF energy harvesting", *IEEE J. Select. Areas Commun.,* vol. 33, no. 8, pp. 1693-1705, Jan. 2015.

[40] S. Boyd and L. Vandenberghe, *Convex Optimization,* Cambridge University Press, 2004.

[41] R. Jain, A. Durresi and G. Babic, "Throughput fairness index: An explanation", ATM Forum Document Number: ATM Forum/990045, Feb. 1999.

[42] N. Zlatanov, A. Ikhlef, T. Islam and R. Schober, "Buffer-Aided Cooperative Communications: Opportunities and Challenges", *IEEE Commun. Mag.,* vol. 52, no. 4, pp. 146-153, Apr. 2014.